Minimal chaos, stochastic webs, and structures of quasicrystal symmetry

G. M. Zaslavskiĭ, R. Z. Sagdeev, D. A. Usikov, and A. A. Chernikov

Institute of Space Research, Academy of Sciences of the USSR

Usp. Fiz. Nauk **156**, 193–251 (October 1988)

The relationship between the problem of the symmetry of a plane tiling and the properties of nonintegrable dynamic systems is reviewed. The formation of stochastic layers and a stochastic web in the motion of linear and nonlinear oscillators subjected to a perturbation is discussed in detail. Emphasis is placed on research on the symmetry properties of a stochastic web with a fractal structure of a quasicrystal type. Structures with a quasicrystal symmetry form as a result of an interaction of two types of symmetries: translational and rotational. Various characteristics of structures with a quasicrystal symmetry are discussed: the distributions of stable and unstable points, the state density, and the Fourier spectrum. Quasicrystal structures in solid state physics, hydrodynamics, botany, and ornamental art are discussed.

CONTENTS

INTRODUCTION

After nearly twenty years of intense research on chaos, we have grown accustomed to the idea that we must always be prepared for surprises in this field of analysis. The chaos phenomenon itself was so unusual for the stereotypes of thought which had become established that a serious effort was required in order to perceive the possibility that low-dimensionality systems could be in a state of chaotic motion without being subjected to random forces. Part of the explanation here is that in order to reach an understanding of just what chaos is it was necessary to find answers to a long list of questions at once. In the course of finding answers to these questions, we have also run into some new and unusual properties of very simple dynamic systems, and we have witnessed the appearance of some new and unusual problems.

Research on certain subtle properties of chaos has now unexpectedly linked the phenomenon of the diffusion of particles to the problem of the symmetry of the tilings of a space. The path of a particle is capable of describing an unusually complex structure in the arrangement of atoms, called a "quasicrystal structure." It turns out that the methods of nonlinear dynamics can reduce many of the symmetry problems of the physics of crystals to a study of the properties of certain mappings which can be established quite simply. Further development of these ideas leads to even more-unexpected interrelationships, since it establishes a correspondence between the structural properties of crystals and quasicrystals, on the one hand, and hydrodynamic structures (e.g., Benard cells), on the other.

The present review is devoted to an analysis of these interrelationships. The penetration of dynamic methods into symmetry theory is not itself unexpected. For example, we quote Weyl's comments on this subject: We still share his (Kepler's) belief in a mathematical harmony of the universe. It has withstood the test of ever-widening experience. But we no longer seek this harmony in static forms like the

 0038-5670/88/100887-29$01.80

regular solids, but in dynamic laws.[26] The actual realization of these ideas, however, is not so simple. The example related to quasicrystal symmetry turns out to be particularly instructive in this regard. Primitive tilings of a plane, in a square or hexagonal grid, are fairly common in nature. There is accordingly nothing surprising about the fact that we frequently find them in nature and, for example, in a hydrodynamic experiment. A quasicrystal symmetry is not so obvious (although it is found fairly frequently in plants). It stems from the real interaction of rotational and translational symmetries. The existence of a dynamic model for this interaction makes it possible to take a considerably broader look at both the properties of dynamic systems and the properties of structures.

The not altogether ordinary analogies which constitute the subject of this review have yet another quality which we should not fail to mention. Structures form in the phase plane in invariant sets: stochastic layers. The thinner the layers, the more regular the structures. The most unusual point here, however, is that a single stochastic path forms a nearly regular structure in the phase plane. The long-range order in the phase plane originates from a chaotic motion.

Our review is organized as follows. In §1 we present a detailed description of the overall picture of the formation of stochastic layers as nucleating regions of a chaos, and we discuss various consequences of this phenomenon, including Arnol'd diffusion. In §2 we consider degenerate cases, in which a stochastic web can appear in phase space with a minimal dimensionality (with 3/2 degrees of freedom). In §3 we use the example of a resonance of a particle with a wave packet in a static magnetic field to introduce a mapping with a twisting, which generates a uniform web with a quasicrystal symmetry. In §4 we discuss various structural properties of the web, and we find an average Hamiltonian of the structures. In §5 we discuss some other applications of quasicrystal structures (in hydrodynamics, botany, and ornamental art).

1. FORMATION OF A STOCHASTIC LAYER

In Hamiltonian systems a region of phase space near a separatrix plays a fundamental role in the analysis of the onset of chaos. In the simplest case of a single degree of freedom, the separatrix is a special path which passes through an unstable saddle point, where it is intersected by another separatrix or intersects itself. A perturbation of the system can be both weak and slow and can thus have a rather weak effect on the dynamics of the system. However, the effect of the perturbation always turns out to be marked if the initial conditions of the system belong to some region near the separatrix. It is in this region that chaos originates, radically changing the properties of the system and rendering it nonintegrable in principle.

The formation of a complex dynamic picture near a separatrix, due to a "splitting" of the separatrix, was pointed out some time ago by Poincaré.[1] The first estimate of the width of the splitting of separatrices was given in Ref. 2. The existence of a stochastic dynamics near a separatrix was described in Ref. 3–5, and the width of a stochastic layer was analyzed for various perturbation cases. The idea of constructing a mapping near a separatrix based on the properties of a path of the system is described in Ref. 4. The relationship between nonintegrability and the existence of a stochastic layer is discussed in Ref. 6. In the discussion below we are following the method developed in Refs. 4, 7, and 8.

1.1. Stochastic layer of a nonlinear pendulum

A nonlinear pendulum is a system which is typical of many physical problems. Its Hamiltonian is

$$H_0 = \frac{1}{2} p^2 - \omega_0^2 \cos x, \tag{1.1}$$

where x is a dimensionless coordinate, p is the momentum, and ω_0 is the small-oscillation frequency of the pendulum. The mass of the pendulum has been set equal to unity. The perturbed problem in its simplest form can be written

$$H = H_0 + V = \frac{1}{2} p^2 - \omega_0^2 \cos x + \varepsilon \frac{\omega_0^2}{k} \cos (kx - \Delta\omega t),$$
$$V \equiv \varepsilon \frac{\omega_0^2}{k} \cos (kx - \Delta\omega t), \tag{1.2}$$

where ε is a dimensionless parameter of the perturbation, and k and $\Delta\omega$ are respectively the wave number and frequency of the perturbation. Hamiltonian (1.2) generates the equation of motion

$$\ddot{x} + \omega_0^2 \sin x = \varepsilon\omega_0^2 \sin (kx - \Delta\omega t). \tag{1.3}$$

Figure 1a is a phase portrait of the unperturbed version of problem (1.3), with $\varepsilon = 0$. If the perturbation is slight (Fig. 1b), some of the invariant paths near the separatrix are disrupted, and a stochastic layer is formed. An estimate of the width of this layer is based on the following considerations.

At small oscillation amplitudes of the pendulum, the pendulum may be regarded as linear ($\sin x \approx x$). The oscillation spectrum of the pendulum thus consists of a single harmonic with the frequency ω_0. In general, the nonlinear frequency of the pendulum, $\omega(E)$, depends on its energy $E = H_0$. At low values of E the frequency is $\omega \approx \omega_0$. A special path—a separatrix—corresponds to the energy $E_c = \omega_0^2$. As $E \to E_c$ the frequency tends toward zero, $\omega(E) \to 0$, and the oscillation period becomes infinite:

$$T = \frac{2\pi}{\omega(E)} \to \infty \quad (E \to E_c = \omega_0^2). \tag{1.4}$$

The typical number of harmonics in the spectrum of a pendulum,

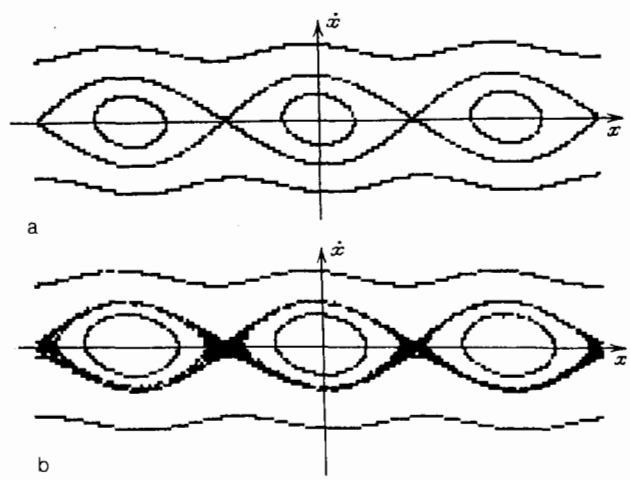

FIG. 1. Phase portrait of a nonlinear pendulum. a—In the absence of a perturbation; b—in the presence of a perturbation. Regions of chaotic dynamics near a separatrix can be seen.

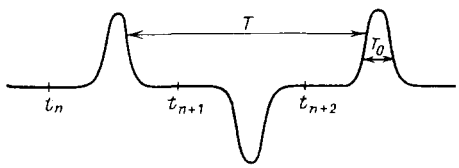

FIG. 2. Time evolution of the velocity of a pendulum for a path near a separatrix. T—Period of the oscillations on the path; T_0—period of small oscillations.

$$N \sim \frac{\omega_0}{\omega(E)} = \frac{T}{T_0} \quad \left(T_0 = \frac{2\pi}{\omega_0}\right), \tag{1.5}$$

tends toward infinity. It follows from property (1.4) that the velocity of the pendulum, $p = \dot{x}(t)$, has the form shown in Fig. 2 at values of E near E_c. The reason that the velocity behaves in this way is that the system traverses nearly the entire width of the potential well quickly (in a time $\sim T_0$) and stays near the saddle points for a long time ($\sim T \gg T_0$). The condition $N \gg 1$ near the separatrix thus makes it possible to switch from a differential equation to a finite-difference equation (a mapping) in perturbed problem (1.3).

It is written between two successive times t_n and t_{n+1} (Fig. 2), taken near the nth and the $(n+1)$ st passages near any of the hyperbolic points. From the equation

$$\dot{E} = \varepsilon\omega_0^2 \dot{x} \sin(kx - \Delta\omega t), \tag{1.6}$$

which is found by differentating $E = H_0$ and using expressions (1.1)–(1.3), we see that a change in the energy of the pendulum occurs only in a region in which its velocity $\dot{x}$ is nonzero. Such a region has a narrow time interval $\sim T_0 = 2\pi/\omega_0$ (Fig. 2) and is equivalent to the brief application of a force to the pendulum. The time interval which elapses between successive "kicks" of this sort is

$$\Delta t_n = t_{n+1} - t_n,$$

and it satisfies the condition that the collision is "instantaneous": $T_0 \ll \Delta t_n$. The mapping which we need thus takes the form, in the case $E < E_c = \omega_0^2$, for example,

$$\begin{aligned} E_{n+1} &= E_n + \Delta E_n, \\ t_{n+1} &= t_n + \frac{\pi}{2}\left(\frac{1}{\omega_n} + \frac{1}{\omega_{n+1}}\right), \end{aligned} \tag{1.7}$$

where

$$\omega_n \equiv \omega(E_n).$$

An expression for ΔE is derived in Appendix 1. Using that expression, and introducing the phase $\theta_n = \Delta t_n$ for convenience, we can finally replace (1.7) in the case $k = 1$ by

$$\begin{aligned} \tilde{E}_{n+1} &= \tilde{E}_n - \frac{4\pi\varepsilon\nu^2 e^{\pi\nu/2}}{\operatorname{sh}(\pi\nu)} \sin\theta_n, \\ \theta_{n+1} &= \theta_n + \nu \ln\frac{32}{\tilde{E}_{n+1}}, \end{aligned} \tag{1.8}$$

where

$$\begin{aligned} \nu &= \frac{\Delta\omega}{\omega_0}, \quad \omega(E) \approx \omega_0 \ln\frac{32}{E}, \\ \tilde{E} &= 1 - \frac{E}{\omega_0^2} = \frac{E_c - E}{E_c}. \end{aligned} \tag{1.9}$$

The simplest estimate of the region of stochastic behavior is found from the inequality[7]

$$\left|\frac{\delta\theta_{n+1}}{\delta\theta_n} - 1\right| > 1. \tag{1.10}$$

For the energy width of the stochastic layer we thus find from (1.8)

$$|\tilde{E}_s| < \frac{4\pi\varepsilon\nu^3 e^{\pi\nu/2}}{\operatorname{sh}(\pi\nu)}. \tag{1.11}$$

If the perturbation in (1.2), (1.3) has a low frequency $\Delta\omega \ll \omega_0$, we have

$$|\tilde{E}_s| < 4\nu^2\varepsilon, \tag{1.12}$$

and the width of the stochastic layer is at a maximum in this case. If, on the contrary, the perturbation has a high frequency ($\Delta\omega \gg \omega_0$), then

$$|\tilde{E}_s| < 8\pi\varepsilon\nu^3 \exp\left(-\frac{\pi\nu}{2}\right), \tag{1.13}$$

and the width of the stochastic layer is exponentially small.

1.2. Interaction of resonances

We will need this simple example in the discussion below. An "interaction of resonances" means the case in which two harmonics, with approximately equal amplitudes and periods but different phase velocities, act on a free particle. The Hamiltonian is

$$H = \frac{1}{2}p^2 - \omega_0^2 \cos x - \omega_0^2 \cos(x + \Delta\omega t). \tag{1.14}$$

If $\Delta\omega \sim \omega_0$, the separatrix cells overlap in the phase plane, and a large region of strong chaos appears.[8] In the case $\Delta\omega \gg \omega_0$, however, the parameter ν is large, and as a result the stochastic layer is thin. A comparison of (1.14) and (1.2) yields $\varepsilon = 1$ and $k = 1$. Our estimate of the layer width in (1.13) then becomes

$$|\tilde{E}_s| < 8\pi\nu^3 \exp\left(-\frac{\pi\nu}{2}\right). \tag{1.15}$$

In other words, two greatly separated resonances ($\Delta\omega \gg \omega_0$) induce exponentially narrow stochastic layers in each other.

1.3. Stochastic layer of a rotator

A "rotator" is a system with a Hamiltonian $H_0 = p^2/2$ which is defined in a cylindrical phase space $x \in (0, 2\pi)$, $p \in (-\infty, \infty)$ and $f(x = 0, p) = f(x = 2\pi, p)$ for an arbitrary function f. The quantities (p, x) represent an angular momentum and a phase. Many problems lead to a perturbed rotator with a Hamiltonian[7-9]

$$\begin{aligned} H &= \frac{1}{2}p^2 - \omega_0^2 \sum_{n=-\infty}^{+\infty} \cos(x - n\Delta\omega t) \\ &= \frac{1}{2}p^2 - \omega_0^2 T_0 \cos x \sum_{n=-\infty}^{+\infty} \delta(t - nT_0), \quad T_0 = \frac{2\pi}{\Delta\omega}. \end{aligned} \tag{1.16}$$

In it, the rotator is perturbed by a periodic sequence of δ-function pulses.

The equations of motion corresponding to (1.16) can be written as the mapping

$$\begin{aligned} p_{n+1} &= p_n - T_0\omega_0^2 \sin x_n, \\ x_{n+1} &= x_n + T_0 p_{n+1} \pmod{2\pi}, \end{aligned} \tag{1.17}$$

where the times are $t_n = nT_0 - 0$. This mapping is also called a "standard mapping" or "Chirikov mapping."[8] Under the condition

$$K = \omega_0^2 T^4 \gtrsim 1, \tag{1.18}$$

system (1.16) becomes highly stochastic, with the result that there is diffusion of particles which is not bounded in p. If $K < 1$, the stochastic regions are localized in phase space. In particular, under the condition $K \ll 1$ there are exponentially narrow stochastic layers. We can demonstrate this point.

We restrict the original form of H in (1.16) to the terms with $n = 0$ and ± 1:

$$H \approx \frac{1}{2} p^2 - \omega_0^2 \cos x - \omega_0^2 [\cos(x + \Delta\omega t) + \cos(x - \Delta\omega t)]. \tag{1.19}$$

The first two terms correspond to the pendulum Hamiltonian H_0 given in (1.1). The last two terms give a perturbation which is analogous to (1.14). They correspond to a weak interaction of resonances, by virtue of the condition $\omega_0/\Delta\omega \ll 1$. The sign of $\Delta\omega$ in (1.19) is unimportant, so we can immediately use (1.15) for the width of the stochastic layer in (1.19):

$$|\tilde{E}_s| < 16\pi\nu^3 \exp\left(-\frac{\pi\nu}{2}\right), \tag{1.20}$$

If we were to take the terms with, for example, $n = \pm 2$ into account in sum (1.16), we would find not $-\pi\nu/2$ but simply $-\pi\nu$ in the argument of the exponential function in (1.20). Since we have $\nu \gg 1$, such terms and also terms with $n > 2$ contribute negligibly.

Figure 3 shows some examples of phase portraits of problem (1.16) or (1.17) under the conditions $K < 1$ and $K > 1$. In addition to the main stochastic layer in the case $K < 1$ there are an infinite number of considerably narrower layers, which result from a disruption of the separatrices from resonances of higher orders. We will pursue the discussion of this example a bit further on.

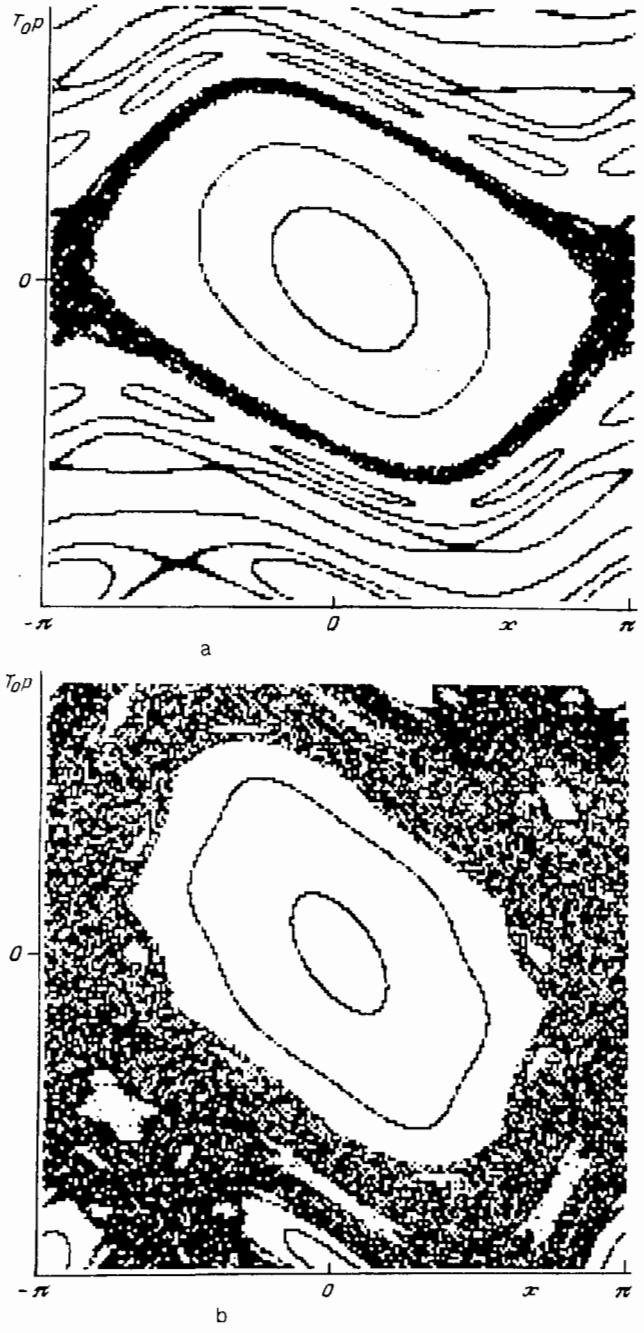

FIG. 3. Phase portraits generated by a standard mapping. a—$K = 0.8$; b—$K = 1.3$.

1.4. Nontrivial discretization effects

The preceding example is very convenient for discussing one of the very serious questions which arise during a stage of escalating use of numerical methods for solving various problems in natural science. Numerical analysis is based on difference schemes, and for this reason we are obliged to switch from differential equations to finite-difference equations. For example, the equation of motion of a pendulum,

$$\ddot{x} + \omega_0^2 \sin x = 0, \tag{1.21}$$

is replaced in the simplest version by the equation

$$x_{n+1} - 2x_n + x_{n-1} + \omega_0^2 (\Delta t)^2 \sin x_n = 0, \tag{1.22}$$

where Δt is the length of the time interval which is the elementary step of the difference scheme, and $x_n = x(n\Delta t)$. To improve the accuracy of calculations, one chooses very small values of Δt. Consequently, the following inequality holds:

$$K = \omega_0^2 (\Delta t)^2 \ll 1. \tag{1.23}$$

To what extent can we control the errors in the switch from problem (1.21) to problem (1.22)? This is of course not a new question. The very first numerical simulations of nonlinear physical problems began the discussion of just what is lost and just what is added by introducing a discretization in a continuous problem.[10] To a large extent, we became able to answer questions of this sort[82] only after it became clear that chaos is possible in dynamic systems. The example of discretization of Eq. (1.21) shows why this is so, and it reveals some nontrivial effects of discretization.

We introduce

$$p_n = \frac{1}{\Delta t}(x_n - x_{n-1}). \tag{1.24}$$

Equations (1.22) and (1.24) can be written as the mapping

$$p_{n+1} = p_n - \omega_0^2 \Delta t \sin x_n, \quad x_{n+1} = x_n + \Delta t p_{n+1} \pmod{2\pi}, \tag{1.25}$$

which is the same as (1.17). We can thus say at the outset that the discrete analog of the equation of motion of a pendulum has stochastic regions regardless of the discretization

step Δt, while the original equation, (1.21), is exactly integrable. In particular, this conclusion means that the switch to discrete equations of motion (1.22) is equivalent to adding a periodic external force due to the discretization.

It is not difficult to find an expression for the force due to the discretization. For this purpose we note that mapping (1.25) is generated by Hamiltonian (1.16), in which we should set $\Delta\omega = 2\pi/\Delta t$. Under condition (1.23), it is sufficient to restrict the sum to the first terms, with $n = 0$ and ± 1; we arrive at Hamiltonian (1.19). We can thus immediately write the Hamiltonian of the discrete problem:

$$H = H_0 + V_{\text{discr}},$$

where H_0 is the Hamiltonian of the original problem, (1.21), and

$$V_{\text{discr}} = -2\omega_0^2 \cos x \cos \frac{2\pi t}{\Delta t} \tag{1.26}$$

is a "discretization potential." This potential is a high-frequency perturbation with an amplitude of the same order as H_0. All the rest of the analysis is obvious, since the phase portrait of discrete problem (1.25) is known (Fig. 3a). All the changes from the simple phase portrait of a pendulum which must be made because of the discretization follow from this phase portrait.

It is now clear that in general a discretization will generate some nonremovable chaotic zones, and a determination of these zones bears directly on the nontrivial discretization effects.

1.5. The KAM theory and Arnol'd diffusion

The Kolmogorov-Arnol'd-Moser theory[11] (the KAM theory) determines the conditions under which the invariant tori of Hamiltonian systems are conserved when a small perturbation acts on a system. If a system with N degrees of freedom is described by the Hamiltonian

$$H_0 = H_0(I_1, \ldots, I_N),$$

which depends on N integrals of motion (actions) I_k, which commute and are independent, then the path of the system lies on an N-dimensional torus.[1]) The torus itself is an invariant. The perturbed Hamiltonian of the system can be written

$$H = H_0(I_1, \ldots, I_N) + \varepsilon V(I_1, \theta_1; \ldots; I_N, \theta_N), \tag{1.27}$$

where the phases θ_k are the canonical conjugates of I_k, and ε is a small perturbation parameter. At sufficiently small values of ε, and in the absence of a degeneracy, i.e., under the condition

$$\text{Det}\left|\frac{\partial^2 H_0}{\partial I_k\, \partial I_l}\right| \neq 0, \tag{1.28}$$

most of the invariant tori are conserved in a slightly deformed state. Some of the tori are disrupted in the process, but the number of disrupted tori is small, and they are squeezed between invariant tori.

This result is illustrated well by Fig. 3a. A system of the type in (1.14) or (1.16) may be thought of as a system with $N = 3/2$. Half-degrees of freedom are also assigned to the periodic external perturbation. A torus is positioned in phase space in such a way that its axis is the time; closure along the axis occurs at the period of the perturbation, T_0; and the (p, x) plane is perpendicular to the axis. Invariant curves in the (p, x) plane lie in the cross section of the invariant torus. Disrupted tori correspond to stochastic layers. In the case $N = 3/2$ or $N = 2$, with $K \ll 1$, the phase space has a complex structure, in which stochastic layers do not intersect.

The possibility of an intersection of stochastic layers in weak interaction with each other exists only at $N > 2$. As a result, the phase space becomes tiled with a network of interconnected narrow channels within which the dynamics of the particles is stochastic. The particles can move away an arbitrarily long distance along this network; this phenomenon has been labeled "Arnol'd diffusion"[12] (Fig. 4). At $N = 2$ the condition for a resonance in the system is

$$n_1\omega_1 + n_2\omega_2 = 0, \tag{1.29}$$

where n_1 and n_2 are integers, and the frequencies of each of the degrees of freedom, ω_i, are given by the known expressions[11]

$$\omega_i = \frac{\partial H_0}{\partial I_i} = \omega_i(I_1, \ldots, I_N) \quad (i = 1, \ldots, N). \tag{1.30}$$

At $N = 2$, condition (1.29) leads to a linear relationship between ω_1 and ω_2. The surface of a given energy $H_0 = E$ thus intersects the family of straight lines $\omega_1/\omega_2 = \text{const}$ at points (Fig. 4a). Near these points, the invariants are violated, and chaos appears. Small perturbations, however, create small regions of chaos, which are not connected to each other. At $N > 2$, such a connection becomes possible (Fig. 4b), and as a result a network which we will call a "stochastic web" arises.

2. MINIMAL CHAOS AND THE STOCHASTIC WEB

The problem of minimal chaos is one of determining the conditions under which small regions of stochastic dynam-

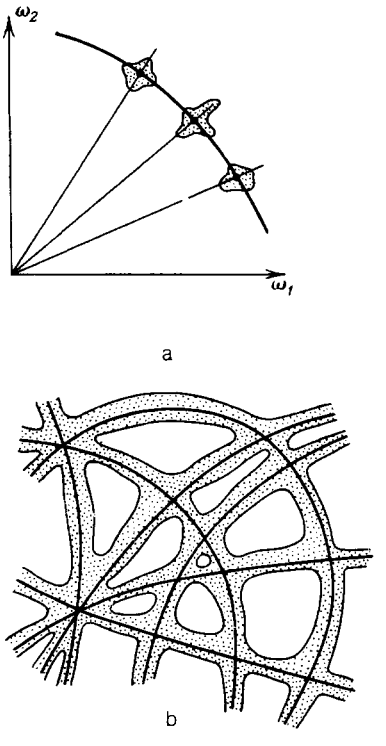

FIG. 4. Stochastic regions for (1) $N = 2$ and (b) $N > 2$.

ics arise from an arbitrarily small perturbation. The existence of minimal chaos implies that the system is nonintegrable in principle, and there is the possibility of a transition from minimal chaos to global chaos, which spans a significant region in the phase space, as some perturbation parameter increases. Two coupled nonlinear oscillators with a Hamiltonian

$$H = H_1(I_1) + H_2(I_2) + \varepsilon V(I_1, \theta_1; I_2, \theta_2)$$

constitute a simple example in which there generally exists minimal chaos at an arbitrarily small value of ε.

A stochastic web is a peculiar manifestation of minimal chaos. The phase space breaks up into separate cells: structures which are separated from each other by stochastic layers. In other words, the web forms in phase space a mosaic of a tiling of the phase space. The length scale of the elementary mosaic structure determines not only the region in which invariant tori exist but also their minimum dimensions. It is thus interesting to determine the conditions under which a stochastic web exists for at least the following reasons: 1) for determining whether a diffusion can occur along the channels of the web at arbitrarily small values of ε, 2) for determining an upper limit on the diameter of the invariant tori at arbitrarily small values of ε, and 3) as an explanation of the internal symmetry of the phase space of the system which arises at arbitrarily small values of ε.

These questions are discussed below.

2.1. Perturbation of a linear oscillator

Certain physical models are quite universal. An example is the perturbed nonlinear oscillator which was introduced in Eqs (1.2) and (1.3). Its Hamiltonian contains two plane waves. This model can be used to explain the fundamental and typical properties of the formation of a stochastic layer. On the other hand, equations like (1.2) and (1.3) arise in many physical applications, so the latter equations can be classified as "standard" equations.

We introduce yet another standard equation:

$$\ddot{x} + \omega_0^2 x = \varepsilon\omega_0^2 \sin(kx - \Delta\omega t), \tag{2.1}$$

which describes a linear oscillator perturbed by a plane wave. The Hamiltonian which leads to (2.1) is

$$H = \frac{1}{2}p^2 + \frac{1}{2}\omega_0^2 x^2 + \varepsilon\frac{\omega_0^2}{k}\cos(kx - \Delta\omega t). \tag{2.2}$$

It arises, particular, in the motion of a charged particle in a static magnetic field B_0 (directed along the z axis) and in the field of an electromagnetic plane wave which is propagating along the x axis.[13-15] Problem (2.1) has been studied extensively[16-18] in connection with the problem of a wave-particle resonance. The perturbation contains a nonlinearity, which, expanded in a Fourier series, leads to a large number of harmonics. Resonances are possible between these harmonics and the frequency of the external perturbation, $\Delta\omega$:

$$n\omega_0 = \Delta\omega, \tag{2.3}$$

where ω_0 has the meaning of a Larmor frequency ($\omega_0 = eB_0/mc$). A specific feature of problem (2.2) is that its unperturbed part is linear. For this reason, if condition (2.3) holds then nondegeneracy condition (1.28) will not hold, and the KAM theorem is immediately inapplicable. The result is the formation of a stochastic web.[19]

2.2. Simplest structure of a stochastic web

We are interested in the case which is near exact resonance (2.3) at a certain value $n = n_0$. We introduce a canonical change of variables:

$$x = \left(\frac{2n_0 I}{\omega_0}\right)^{1/2}\cos\left(\frac{\varphi}{n_0} - \Delta\omega t\right),$$

$$p = (2n_0 I\omega_0)^{1/2}\sin\left(\frac{\varphi}{n_0} - \Delta\omega t\right), \tag{2.4}$$

where (I, φ) are action-angle variables.

Hamiltonian (2.2) is transformed by (2.4) to

$$H = (n_0\omega_0 - \Delta\omega)I + \varepsilon\frac{\omega_0^2}{k}\sum_n J_n(k\rho) \times \cos\left[\frac{n}{n_0}\varphi + \left(\frac{n}{n_0} - 1\right)\Delta\omega t\right], \tag{2.5}$$

where $J_n(k\rho)$ are Bessel functions, and the quantity

$$\rho = \left(\frac{2n_0 I}{\omega_0}\right)^{1/2} \tag{2.6}$$

has the meaning of a Larmor radius if we take ω_0 to be a Larmor frequency.

The purpose of the introduction of variables (2.4) is to separate the slow motion from the fast motion near the resonance. At exact resonance (2.3), we write (2.5) in the form

$$H = H_0 + V, \tag{2.7}$$

$$H_0 = \varepsilon\frac{\omega_0^2}{k}J_{n_0}(k\rho)\cos\varphi,$$

$$V = \varepsilon\frac{\omega_0^2}{k}\sum_{n\neq n_0} J_n(k\rho)\cos\left[\frac{n}{n_0}\varphi + \left(\frac{n}{n_0} - 1\right)\Delta\omega t\right].$$

The situation which arises here has already been encountered, in the preceding section of this paper. The unperturbed motion is described by the Hamiltonian H_0. This motion has some singular paths or separatrices, which are disrupted by the perturbation V, with the result that stochastic layers form.

The singular points are found from the conditions

$$\frac{\partial H_0}{\partial I} = 0, \quad \frac{\partial H_0}{\partial\varphi} = 0.$$

The hyperbolic points (ρ_*, φ_*) are defined by the equations

$$J_{n_0}(k\rho_*) = 0, \quad \varphi_* = \pm\frac{\pi}{2}, \tag{2.8}$$

and the family of elliptical points (ρ_0, φ_0) are defined by the equations

$$J'_{n_0}(k\rho_0) = 0, \quad \varphi_0 = 0, \pi. \tag{2.9}$$

The family of separatrices which pass through points (2.8) have the structure of a web (Fig. 5). This web consists of $2n_0$ rays and concentric circles with radii $\rho_*^{(s)}$ in the (x, p) plane, where the $k\rho_*^{(s)}$ are various roots of the Bessel function J_{n_0}. To reach an understanding of the physical situation, it is sufficient to consider only the case of high particle energies, $k\rho_0 \gg n_0$. We can then write

$$H_0 = \pm\varepsilon\frac{\omega_0^2}{k}\left(\frac{2}{\pi k\rho_0}\right)^{1/2}\cos k\tilde{\rho}\cdot\cos\varphi, \tag{2.10}$$

where $\tilde{\rho} = \rho - \rho_0 \ll \rho_0$, and the choice of sign depends on the phase of the elliptical point with coordinates (2.9).

The period of the oscillations of the particles within one cell of the separatrix in Fig. 5 is found from (2.10) to be

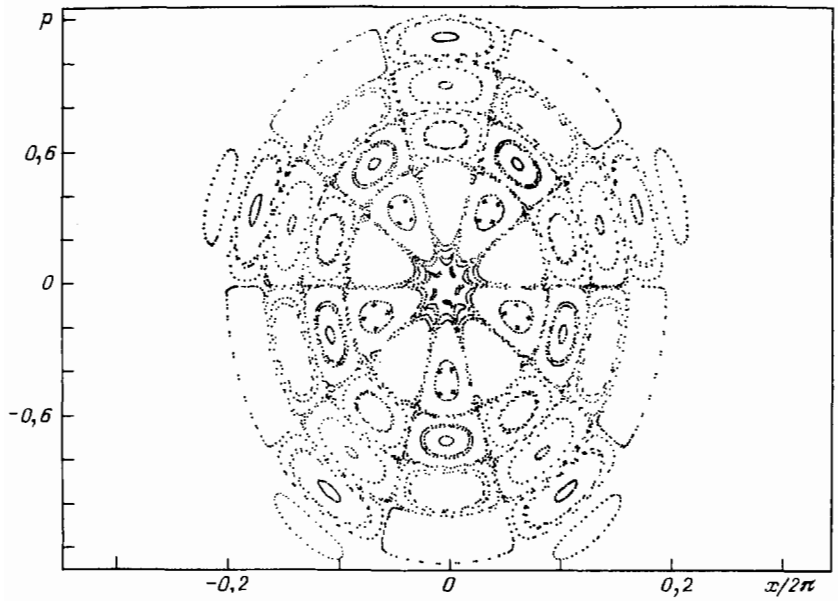

FIG. 5. Phase portrait for Eq. (2.1) in the $(x/2\pi, p)$ plane for $n_0 = 5$, $\varepsilon\omega_0^2/k = 1/80$, $k = 15$. The dots in the plane correspond to the intervals between times of $2\pi/\omega_0$.

$$T = \left(\frac{\pi}{2}\right)^{1/2} \frac{4\Delta\omega}{k\varepsilon\omega_0^2 n_0} (k\rho_0)^{3/2} K(\varkappa), \tag{2.11}$$

where $K(\varkappa)$ is the complete elliptic integral of the first kind, and

$$\varkappa = 1 - \frac{H_0^2 k^2 \pi k\rho_0}{2\varepsilon^2\omega_0^4}. \tag{2.12}$$

Near the equilibrium position within a cell of the web, a particle undergoes small oscillations with a period

$$T_0 = \left(\frac{\pi}{2}\right)^{1/2} \frac{4\Delta\omega}{k\varepsilon\omega_0^2 n_0} (k\rho_0)^{3/2}, \tag{2.13}$$

and for the oscillations of the particles near the separatrix $(H_0 \to 0)$ we have

$$T = \left(\frac{\pi}{2}\right)^{1/2} \frac{4\Delta\omega}{k\varepsilon\omega_0^2 n_0} (k\rho_0)^{3/2} \ln\left[\frac{4\varepsilon\omega_0^2}{k^2 H_0}\left(\frac{2}{\pi k\rho_0}\right)^{1/2}\right], \tag{2.14}$$

and the period diverges logarithmically. This result means that the perturbation V in (2.7) is a high-frequency perturbation ($\Delta\omega T \gg 1$ at sufficiently small values of H_0). This perturbation disrupts the separatrix network and gives rise to a stochastic layer of exponentially small width:

$$E_s = (2\pi)^{3/2} \frac{4\omega_0^2}{k^3\varepsilon n_0^2} (k\rho_0)^{5/2} \exp\left[-\frac{(\pi k\rho_0/2)^{3/2}}{kn_0\varepsilon}\right] \tag{2.15}$$

(see the derivation of this expression in Appendix 2).

An unbounded network of channels thus forms in the phase plane (Fig. 5), and particles can escape along these

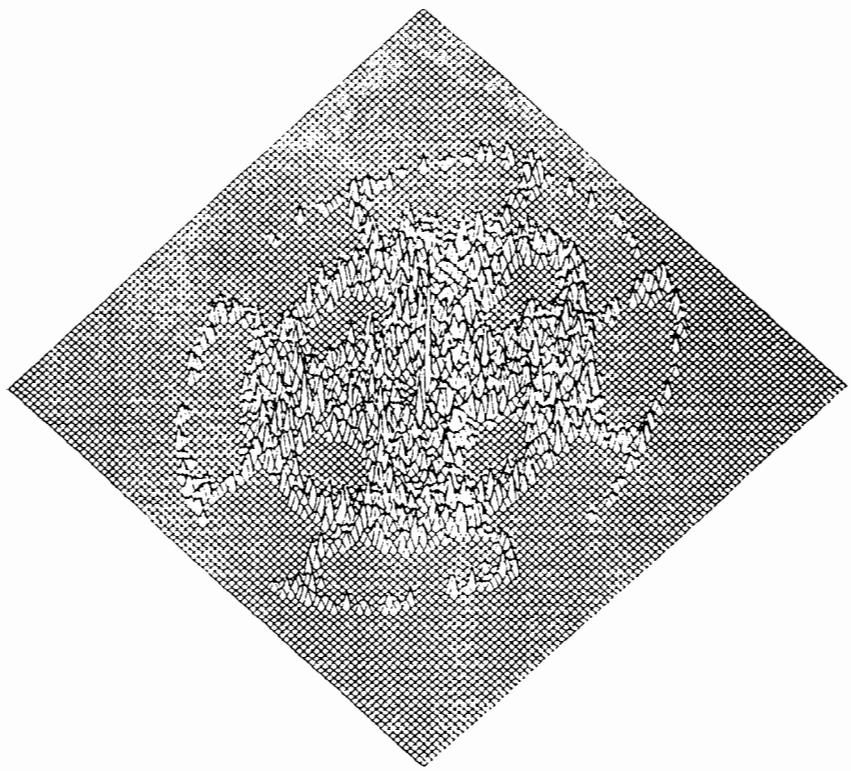

FIG. 6. Distribution function on a stochastic web for Eq. (2.1) with $\varepsilon\omega_0^2/k = 0.1$, $k = 15$, $\Delta\omega = 4\omega_0$ and a computation time $2\cdot 10^4 \cdot 2\pi/\Delta\omega$.

channels. The velocity of the particles increases with distance from the center. At the same time, however, the width of the web decreases. According to expression (2.15), the width of the web falls off exponentially with increasing energy of the particles, since we have $\rho_0 \sim E^{1/2}$ [see definition (2.6)]. Accordingly, although the web is formally unbounded, the probability for the particles to reach the high-energy region by a diffusive penetration is exponentially small. This circumstance is reflected quite well in the form of the distribution function[19] (Fig. 6).

The picture drawn here for the formation of a stochastic web remains valid when we are not very far from the resonance:

$$\delta\omega = n_0\omega_0 - \Delta\omega \neq 0.$$

As a simple estimate of the values of $\delta\omega$ for which the web does not disappear we can use the limitation

$$\delta\omega < \frac{2\pi}{T_0} = \left(\frac{2}{\pi}\right)^{1/2} \frac{k\varepsilon\omega_0^2 n_0}{4\Delta\omega\,(k\rho_0)^{3/2}}.$$

The existence of a stochastic web was found at the lowest possible number of degrees of freedom, $N = 3/2$, at which the system can still be nonintegrable. We can thus assume that in Hamiltonian systems there exists a universal and unbounded embryonic chaos if certain conditions, concerning a sufficiently strong frequency degeneracy, are satisfied.

2.3. Stochastic layers of a nonlinear oscillator

A nonlinearity in a system automatically lifts a strong degeneracy. Resonance conditions may, nevertheless, lead to the retention of a certain part of the web.[19] To find an explanation for this effect, we go back to Eq. (1.3).

At small oscillation amplitudes x the nonlinear oscillator is approximately a linear oscillator. We should therefore expect to see the appearance of elements of a stochastic web in the main cell of the separatrix of a nonlinear oscillator. This is indeed what we do see at sufficiently large values of k and ε, if resonance condition (2.3) holds. A numerical analysis shows[19] that a disrupted separatrix system with a symmetry imposed by the order of the resonance does indeed form at small values of x (Fig. 7). As ε varies, this part of the web changes in structure, undergoing a succession of different bifurcations. The size of the separatrix cells of second order is of the order of $2\pi/k$, i.e., of the order of the perturbation wavelength. An internal structure of this sort is thus possible only at $k > 2$. Between the inner cell of the web and the ordinary stochastic layer in the plane of the main separa-

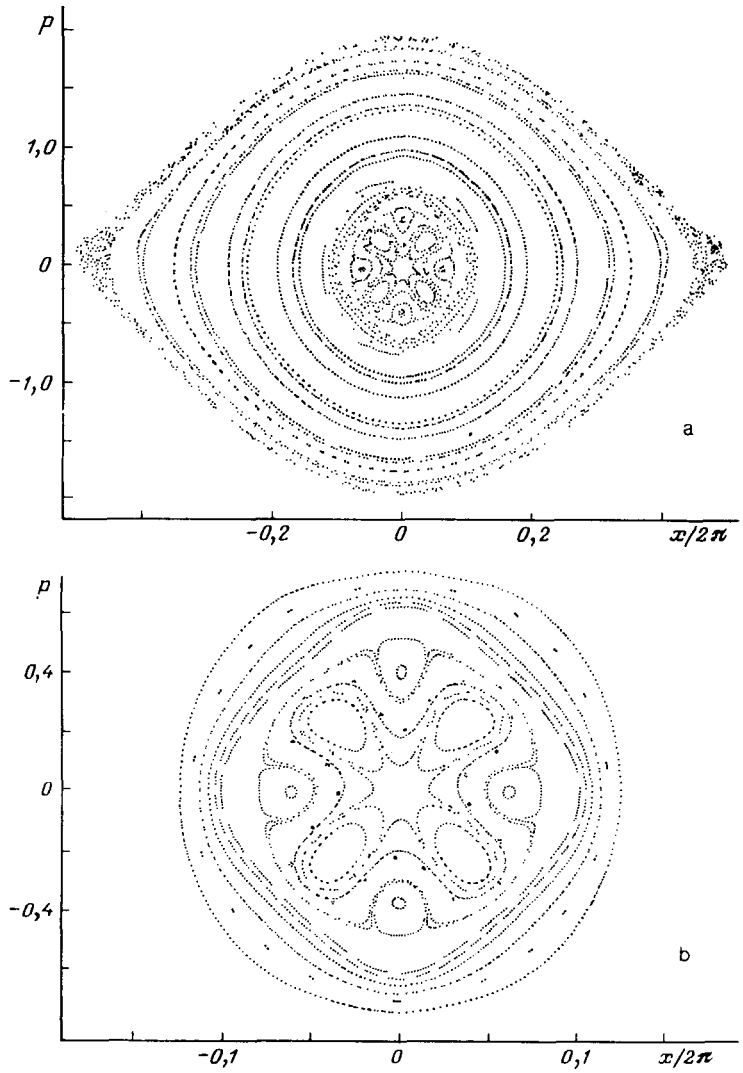

FIG. 7. Phase portrait of perturbed nonlinear oscillator (1.3) under the resonance conditions $\Delta\omega = 4\omega_0$ and $k = 15$, with $\varepsilon = 1/30$. a—General view of one cell of the separatrix; b—details of the inner region of the cell shown in part a.

trix (Fig. 7a) there are ordinary invariant tori, in accordance with the KAM theory.

Consequently, even in the nonlinear case, which lacks an exact degeneracy, an external resonance may cause an anomalous pattern, disrupting the invariant tori and setting the stage for transverse diffusion. The adiabatic invariant for the particles within an element of the web may change substantially.

A similar picture arises in a study of the dynamics of charged particles in the field of an electromagnetic wave which is propagating at a phase velocity equal to the velocity of light ($\omega = kc$) in the direction across a uniform magnetic field[20] (Appendix 3).

3. STOCHASTIC WEB WITH QUASICRYSTAL SYMMETRY

After it became clear that a stochastic web exists in the case of minimal nonintegrable dimensionality of a dynamic system, the problem of determining its possible typical and exceptional cases seemed important. Among the exceptional cases is a web which has a roughly uniform thickness throughout an infinite phase plane. Such a case is possible[5]; it arises in the class of problems which contain wave-particle resonances in a static magnetic field. This case is of particular interest because it is a peculiar generator of a new type of symmetry,[21] which we will be discussing in detail below.

3.1. Mapping with twisting

We again consider an oscillator, but now one which is subjected not to a single plane wave, as in (2.1), but to a packet of an infinite number of plane waves, with identical amplitudes and a constant frequency shift:

$$\ddot{x} + \omega_0^2 x = -\varepsilon\omega_0^2 \sum_{n=-\infty}^{+\infty} \sin(kx - \omega t - n\Delta\omega t). \tag{3.1}$$

It is convenient for the discussion below to set

$$\theta = kx - \omega t$$

and to write (3.1) in the form

$$\ddot{x} + \omega_0^2 x = -\varepsilon\omega_0^2 T_0 \sin\theta \sum_{n=-\infty}^{+\infty} \delta(t - nT_0), \tag{3.2}$$

using the same notation, $\Delta\omega = 2\pi/T_0$. The Hamiltonian of system (3.1) or (3.2) is

$$H = \frac{1}{2}p^2 + \frac{1}{2}\omega_0^2 x^2 - \varepsilon\frac{\omega_0^2}{k} T_0 \cos(kx - \omega t) \sum_{n=-\infty}^{+\infty} \delta(t - nT_0). \tag{3.3}$$

The physical meaning of this Hamiltonian can be seen easily by comparing this case, (3.1)–(3.3), with two problems which we have already discussed, (1.16) and (2.2). Instead of the smooth periodic perturbation as in (2.2), the oscillator is subjected to periodic δ-function pulses, i.e., instantaneous "kicks," as in the problem of a perturbed rotator (1.16). Furthermore, Eq. (3.3) corresponds to a plane motion of a charged particle in a static magnetic field $B_0 \perp z$ and in an electrostatic field directed along the x axis:

$$E(x, t) = -\varepsilon\omega_0^2 T_0 \sin\theta \sum_{n=-\infty}^{+\infty} \delta(t - nT_0). \tag{3.4}$$

The degeneracy can now be particularly pronounced at resonances:

$$\alpha = \omega_0 T_0 = \frac{2\pi p}{q}, \tag{3.5}$$

where p and q are integers (below we will assume simply $p < q$). Resonance condition (3.5) means (for $p = 1$, for example) that over the time taken by a particle to complete an orbit in the magnetic field ($2\pi/\omega_0$) it will be kicked precisely q times by the wave field.

Equation of motion (3.2) can be integrated once; as a result we find a mapping which relates the values of (p, x) after a time interval T_0:

$$\hat{T}:$$
$$p_{n+1} = [p_n + \varepsilon\omega_0^2 T_0 \sin(n\omega T_0 - kx_n)]\cos\alpha - \omega_0 x_n \sin\alpha,$$
$$x_{n+1} = x_n \cos\alpha + \frac{1}{\omega_0}[p_n + \varepsilon\omega_0^2 T_0 \sin(n\omega T_0 - kx_n)]\sin\alpha, \tag{3.6}$$

where $\alpha = \omega_0 T_0$. At $\omega_0 = 0$, mapping (3.6) becomes standard mapping (1.17). The presence of a constant average velocity ω/k for wave packet (3.4) leads to a particle acceleration effect, as we mentioned earlier. A more symmetric case arises at $\omega = 0$. In this case, mapping (3.6) becomes a so-called mapping with a twisting through an angle α (Ref. 5):

$$\hat{M}_\alpha:$$
$$p_{n+1} = (p_n - \varepsilon\omega_0^2 T_0 \sin kx_n)\cos\alpha - \omega_0 x_n \sin\alpha,$$
$$x_{n+1} = x_n \cos\alpha + \frac{1}{\omega_0}(p_n - \varepsilon\omega_0^2 T_0 \sin kx_n)\sin\alpha. \tag{3.7}$$

It is also convenient to introduce the dimensionless variables

$$u = kp/\omega_0; \quad v = -kx \tag{3.8}$$

and to write $\hat{M}_\alpha$ in the form

$$\hat{M}_\alpha:$$
$$u_{n+1} = (u_n + K_H \sin v_n)\cos\alpha + v_n \sin\alpha,$$
$$v_{n+1} = -(u_n + K_H \sin v_n)\sin\alpha + v_n \cos\alpha, \tag{3.9}$$

where

$$K_H = \varepsilon\omega_0 T_0. \tag{3.10}$$

We denote the cases of resonance (3.5) with $p = 1$ by

$$\alpha_q = \frac{2\pi}{q}. \tag{3.11}$$

As we will see below, these cases play a particularly important role. The parameter K_H is a measure of the strength of the interaction of the particle with the waves. If $K_H = 0$, the mapping $\hat{M}_\alpha$ describes a rotation through an angle α over one step.

We can get an idea of the properties of $\hat{M}_\alpha$ by the following qualitative approach: We write the parameter α in the form

$$\alpha = \frac{2\pi p_{(0)}}{q_{(0)}} + \delta\alpha,$$

where $p_{(0)}$ and $q_{(0)}$ are integers, and $\delta\alpha$ is the part of α which is not related to a rationality. Furthemore, we choose $p_{(0)}$ and $q_{(0)}$ in such a way that $q_{(0)}$ is minimized. If we are far from the main resonances, i.e., if $q_{(0)} \neq 1, \ldots n$, where n is an integer and not too small, and if $|\delta\alpha| \lesssim 1/n$, then the mapping (3.9) will be much the same as a standard mapping, regardless of the value of p_0. This result mean that for

$K = \varepsilon\omega_0^2 T_0^2 \gtrsim 1$ there will be strong chaos in it, while at $K < 1$ there will be only some narrow stochastic layers over a significant region of the phase space.

The situation changes when condition (3.11) holds.

3.2. Resonance Hamiltonian

If the parameter K_H is small, we can put Hamiltonian (3.3) in a more convenient form under resonance condition (3.11). Using the notation in (3.5) and (3.8), we rewrite this Hamiltonian as (within a constant factor)

$$H = \frac{1}{2}\alpha_q (u^2+v^2) - K_H \cos v \sum_{n=-\infty}^{+\infty} \delta(\tau - n), \qquad (3.12)$$

where $\tau = t/T_0$. We write (u, v) in polar coordinates:

$$u = \rho \sin \varphi, \quad v = -\rho \cos \varphi,$$

where ρ is a dimensionless Larmor radius. Using the generating function

$$F = (\varphi - \alpha_q \tau) I, \quad I = \frac{1}{2}\alpha_q \rho^2,$$

we transform to a coordinate system which is rotating at a frequency α_q. In terms of the new variables, the Hamiltonian is

$$\tilde{H} = H + \frac{\partial F}{\partial \tau} = -K_H \cos[\rho \cos(\varphi - \alpha_q \tau)] \sum_{n=-\infty}^{+\infty} \delta(\tau - n). \qquad (3.13)$$

We transform the series of δ-functions:

$$\sum_{n=-\infty}^{+\infty} \delta(\tau - n) = \sum_{j=1}^{q} \sum_{m=-\infty}^{+\infty} \delta(\tau - (mq + j)).$$

Substituting this expression into (3.13), and using the representation

$$\sum_{m=-\infty}^{+\infty} \delta(\tau - j - mq) = \frac{1}{q} \sum_{m=-\infty}^{+\infty} \exp\left(2\pi i m \frac{\tau - j}{q}\right),$$

we easily find

$$\tilde{H} = H_q + V_q, \qquad (3.14)$$

$$H_q = -\frac{1}{q} K_H \sum_{j=1}^{q} \cos \xi_j,$$

$$V_q = -\frac{2}{q} K_H \sum_{j=1}^{q} \cos \xi_j \sum_{m=1}^{\infty} \cos\left[\frac{2\pi m}{q}(\tau - j)\right],$$

where

$$\xi_j = -\rho \cos\left(\varphi + \frac{2\pi}{q} j\right) = v \cos\left(\frac{2\pi}{q} j\right) + u \sin\left(\frac{2\pi}{q} j\right). \qquad (3.15)$$

Here $\xi_j = \mathbf{R}\mathbf{e}_j$, where $\mathbf{R}$ is a state vector in the (u, v) phase plane, and $\mathbf{e}_j$ is a unit vector which defines a vertex of a regular q-gon.

We call expression H_q a "resonance Hamiltonian." It determines a certain integrable Hamiltonian system. The second term in $\tilde{H}$ describes a perturbation V_q which acts on H_q. This perturbation, in particular, disrupts the separatrices in H_q, forming narrow regions of chaotic dynamics.[21]

In the more general case, (3.12) would be replaced by the Hamiltonian

$$H = \frac{1}{2}\alpha_q (u^2+v^2) - K_H f(v) \sum_{n=-\infty}^{+\infty} \delta(\tau - n), \qquad (3.16)$$

where $f(v)$ is some arbitrary function. Corresponding to this Hamiltonian is the resonance Hamiltonian

$$H_q = -\frac{1}{q} K_H \sum_{j=1}^{q} f(\xi_j), \qquad (3.17)$$

where the system of vectors

$$\mathbf{e}_j = \left(\cos\frac{2\pi}{q} j, \sin\frac{2\pi}{q} j\right) \quad (j = 1, \ldots, q),$$

onto which the state vector $\mathbf{R} = (u, v)$ is projected, forms a regular "star." In yet another generalization of (3.17), the "star" $\mathbf{e}_j$ could be irregular; i.e., $\mathbf{e}_j$ would be a set of q arbitrarily directed unit vectors.

A distinctive feature of representation (3.14) is the presence of the interaction parameter K_H in the average Hamiltonian H_q and in the time-varying part of V_q. In other words, the reduced Hamoltonian $\tilde{H}$ is proportional to the constant K_H, vanishing in the case $K_H = 0$. The structure of the phase plane for a system with the Hamitonian H_q thus exists only because of the combined effect of the magnetic and electrostatic fields on the particle (in other words, the structure stems from an interaction of the translational and rotational symmetries). The effect of V_q, however, may be either small or large, depending on the relation between the frequency of the perturbation V_q and the unperturbed frequency of the oscillations described by Hamiltonian H_q. This frequency is evidently of the order of K_H and the frequency perturbation of the V_q is of the order of unity. Accordingly, in the case $K_H \ll 1$ a perturbation is always a high-frequency perturbation and leads to small corrections. In the case $K_H \gtrsim 1$, in contrast, we would expect a strong interaction of resonances and the formation of a large region of chaotic dynamics.

The Hamiltonian H_q thus describes the expression for H averaged over the period of the Larmor revolution.

3.3. Trivial resonances

The values $q = 1, 2$ and $q = 3, 4, 6$ correspond to cases of trivial resonances. The reasons will become clear below.

With $q = 1$ we find from (3.14)

$$H_1 = -K_H \cos v. \qquad (3.18)$$

The average Hamiltonian H_q describes a free motion with a momentum v and a periodic dependence of the energy H_q on v. A dispersion law of this type arises, in particular, in periodic lattices. The equations of motion

$$\dot{v} = 0, \quad \dot{u} = K_H \sin v$$

lead to the solution

$$v = \text{const} = v_0, \quad u = u_0 + tK_H \sin v_0. \qquad (3.19)$$

This solution describes an acceleration along the x axis due to a so-called cyclotron resonance; it is the same as the exact solution found from mapping $\hat{M}_\alpha$ in (3.9).

With $q = 2$ we find from (3.14) $H_2 = H_1$; i.e., this case is the same as the preceding case. It corresponds to a half-integer cyclotron resonance (we are assuming $p = 1$ every-

where, although this value can also be arbitrary).

With $q = 4$ we find (Ref. 5)

$$H_4 = -\Omega_4 (\cos v + \cos u), \quad \Omega_4 = \frac{K_H}{2T}, \tag{3.20}$$

$$V_4 = -\Omega_4 (\cos v - \cos u) \cos \pi\tau, \tag{3.21}$$

and the other terms in V_4, which contain $\cos(m\pi\tau)$ with $m > 1$, can be ignored, as we will see below.

The unperturbed motion of a particle is characterized by the Hamiltonian H_4 and the normalized energy integral

$$E_4 = \cos v + \cos u.$$

Corresponding to stable equilibrium positions are the elliptical points

$$|E_4| = 2, \quad v = \pi n, \quad u = \pi m,$$

$$m + n = 2l \quad (l = 0, \pm 1, \ldots).$$

Unstable hyperbolic points are determined by the conditions

$$E_4 = 0, \quad v = \pi n, \quad u = \pi m,$$

$$m + n = 2l + 1 \quad (l = 0, \pm 1, \ldots).$$

The separatrices which pass through them tile the entire phase plane with a square network determined by the equations

$$v = \pm(u + \pi) + 2\pi n \quad (n = 0, \pm 1, \ldots). \tag{3.22}$$

The path of the average motion in the case $|E_4| \leqslant 2$ is

$$\cos v = \frac{1}{2} E_4 + \left(1 - \frac{1}{2} E_4\right) \mathrm{cd}\left[\left(1 + \frac{1}{2} E_4\right) \Omega_4 t;\ \varkappa\right],$$

$$\cos u = \frac{1}{2} E_4 - \left(1 - \frac{1}{2} E_4\right) \mathrm{cd}\left[\left(1 + \frac{1}{2} E_4\right) \Omega_4 t;\ \varkappa\right],$$

where $cd = cn/dn$ is the ratio of elliptic functions with modulus

$$\varkappa = \frac{2 - E_4}{2 + E_4}.$$

Incorporating the next term in the perturbation V_4 in the Hamiltonian $\tilde{H}$ [see (3.18) and (3.20)] leads to a disruption of separatrix network (3.22) and to the formation of a stochastic layer of thickness[5]

$$\Delta H \approx \frac{8\pi^3}{K_H T} \exp\left(-\frac{\pi^2}{K_H}\right). \tag{3.23}$$

The layer now tiles the entire phase space, having a form which is approximately a square network, with a finite uniform thickness ΔH given by (3.23). Figure 8a shows an example of a stochastic web with $q = 4$. It is slightly modulated by the perturbation V_4. The perturbation parameter (which determines the modulation depth) is $\sim\Omega_4^2$. If we had retained the following terms in the perturbation V_4 in (3.21), they would have provided an additive contribution with a decay index higher than that in (3.23). This circumstance justifies our ignoring these terms. With increasing $K_H < 1$, the width of the stochastic web increases. Its modulation depth increases simultaneously. Its shape becomes progressively less similar to a square network, although the symmetry under a rotation through $\pi/2$ is retained. In this manner, a stochastic sea is formed from the web.

At $q = 3$ we find a similar picture (Fig. 8b). The shape

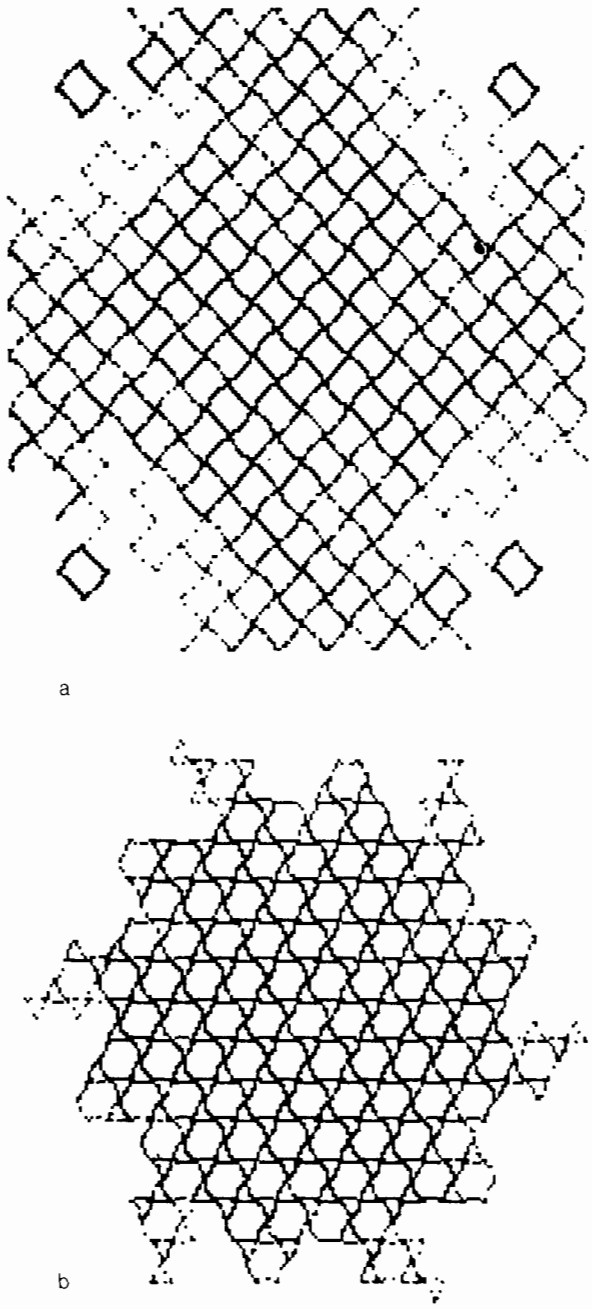

FIG. 8. Stochastic web in the case of "trivial" resonances in the (u, v) phase plane. a—$q = 4$ (square lattice), $K_H = 0.7$, size of square $24\pi \times 24\pi$; b—$q = 3$ ("kagome" lattice), $K_H = 0.8$, size of square $32\pi \times 32\pi$.

of the web formed in this case is called a "kagome lattice," which is associated in some simple way with a honeycomb lattice. The Hamiltonian

$$H_3 = -\frac{1}{3} K_H \left(\cos v + 2 \cos \frac{1}{2} v \cdot \cos \frac{\sqrt{3}}{2} u\right) \tag{3.24}$$

determines the dynamics of the particles, which can produce "triangular" or "hexagonal" invariant curves in the phase plane. They are separated by a separatrix network determined by the equations

$$v = \pi (2n_1 + 1), \quad v = \sqrt{3}\, u + 2\pi (2n_2 + 1),$$

$$v = -\sqrt{3}\, u + 2\pi (2n_3 + 1)$$

$$(n_1, n_2, n_3 = 0, \pm 1, \ldots).$$

These equations create the kagome lattice. On the separatrix network the energy integral

$$E_3 = \cos v + 2\cos\frac{v}{2}\cdot\cos\frac{\sqrt{3}}{2}u \qquad (3.25)$$

has the value $E_3^{(c)} = -1$. For values in the interval $-1 \geqslant E_3 \geqslant -3/2$ the motion of a particle occurs within the triangles of the lattice; for $3 \geqslant E_3 \geqslant -1$, the motion occurs within hexagons. The pattern in Fig. 8b has one unique feature: On the one hand, it is a hexagonal "snowflake," which can be generated through a growth of crystals. On the other hand, we are dealing with a typical Koch fractal,[23] which is not produced by some formal algorithm but is instead "mapped" by the path of the particle in fields of fairly simple configuration: The particle "draws" a fractal in these fields. The case $q = 6$ leads to the same Hamiltonian, (3.24), and thus contains no new information. Consequently, there exist two types of lattices in the plane in the cases $q = 3$ and $q = 4$, which create structures with translational and, simultaneously, rotational symmetry. We know[23] that there are no other structures which have similar symmetry properties. It is for this reason, that all the cases listed above, of resonance Hamiltonians H_q with $q = 1, 2, 3, 4$, and 6, were called "trivial."

They describe very simple structures.

3.4. Nontrivial resonances and a web with quasicrystal symmetry

In all other cases of a resonance, in which q does not take on the values listed above, a nontrivial situation develops. In such cases it is not possible to tile the plane with a network which would have translational and rotational symmetry simultaneously. The new structure of the stochastic web is very specific; it falls in the category of structures having a symmetry of a so-called quasicrystal type. Figures 9a, 9b, and 10 show examples of webs for $q = 5$, 7, and 8. The web is a set of points of a mapping $\hat{M}_q$ over a fixed time interval. The structures in these figures are formed by a random walk of the mapping point in the phase plane. Since the point cannot go outside the channels of the web, we will, over a long time, acquire fairly detailed information about the structure of the web. This structure, however, develops in a very nonuniform way over time. Figure 9a shows a web which is drawn nearly completely over the time it is observed (the computation time). In Fig. 9b we see an entirely different picture. Over more than 10^6 mapping steps, a window remains in the web in the form of a fractal five-point star. The window overgrows the web at times $\tau > 1.3\cdot 10^6$. Windows of various sizes and shape appear, depending on the choice of initial conditions. The order of events in the formation of a "snowflake" from a web is very sensitive to the initial values; this circumstance is in turn related to the existence of Cantor tori,[24] which inhibit certain diffusion directions.

The growth of the web occurs in the following way. First, a random walk of the point in the plane creates some irregular figure, e.g., a star whose points have not all grown to the same extent. The structure of this star then converts into a regular structure, and in the next stage of the growth of the web a large star begins to form. The boundaries of these stars of course have a complex shape, and they form fractal curves in the limit $t \to \infty$. For this reason, we will also call a

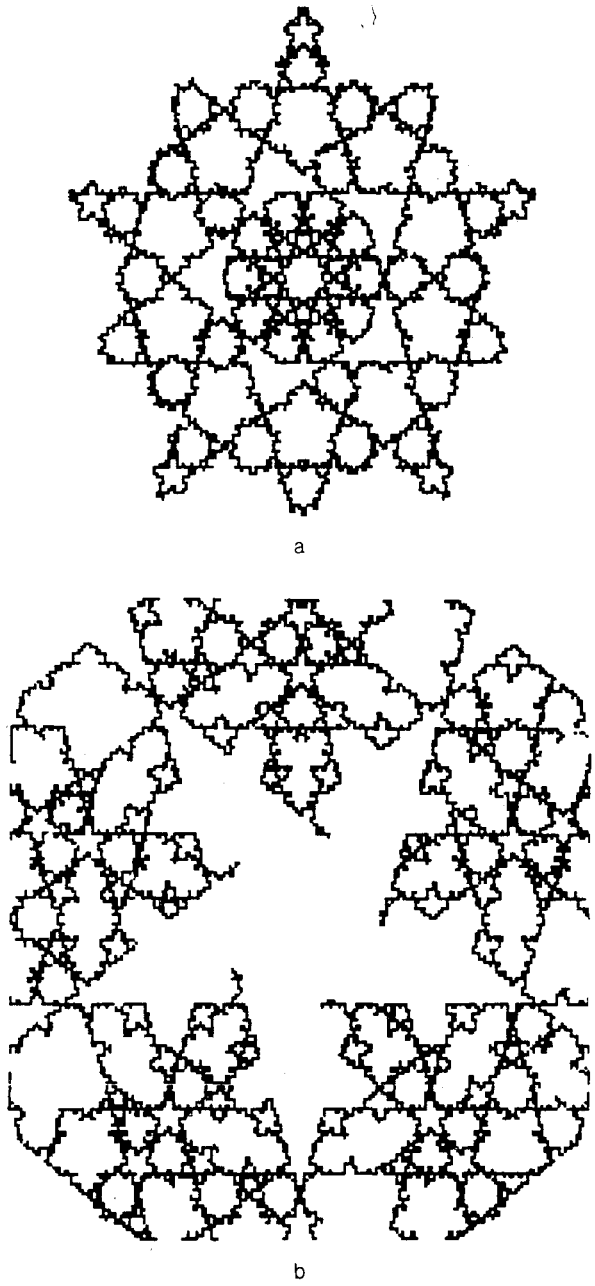

FIG. 9. Stochastic web in the case of a fivefold symmetry ($q = 5$). $K_{II} = 0.7$, size of squares $256\pi \times 256\pi$.

stochastic web with quasicrystal symmetry a "fractal web."

A fractal web has an unclosed central window in the form of a regular q-gon if q is even or a $2q$-gon if q is odd. Inside the central window there are also separatrices and stochastic layers, but these entities do not reach the edge of the window and do not connect with the main web. The reason is that the phase space inside the window has a structure which is most reminiscent of the phase portrait of a standard mapping.[8,16] With decreasing K_H, the size of the central window increases.[5] With decreasing K_H, and also with increasing q, the web becomes thinner, and its cells wider.

3.5. Diffusion of particles in a magnetic field

The problem of a stochastic web has a dynamic aspect as well as a structural one. In particular, the dynamic aspect

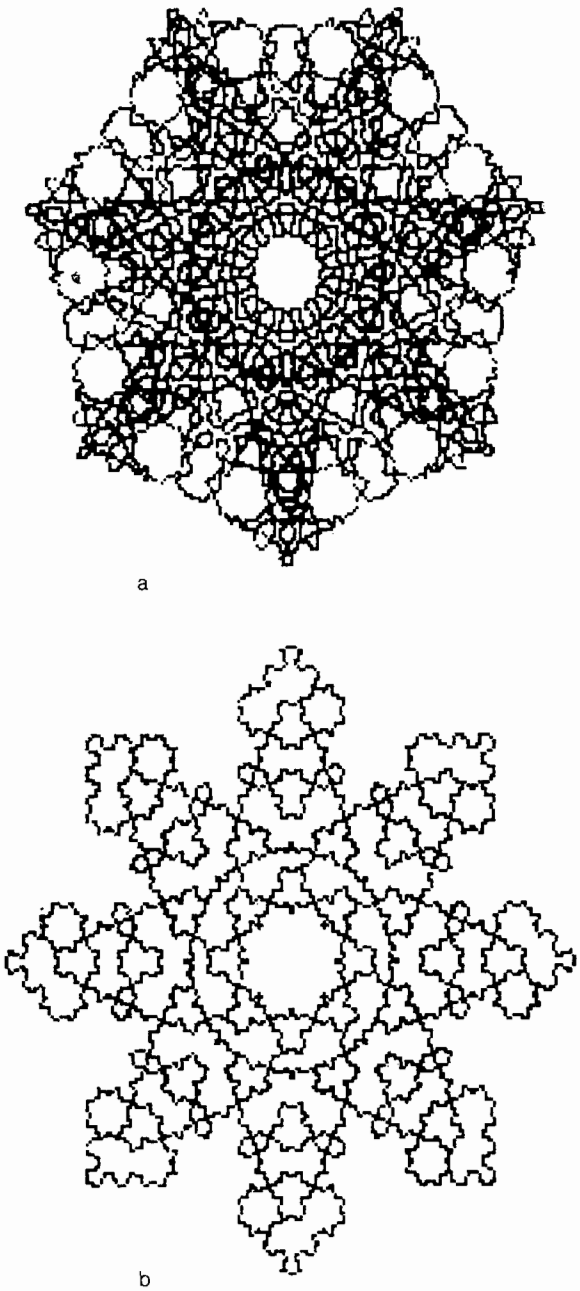

FIG. 10. Stochastic web in the cases of sevenfold and eightfold symmetries. a—q = 7, $K_{II} = 0.5$, size of square $64\pi \times 64\pi$; b—$q = 8$, $K_{II} = 0.6$, size of square $128\pi \times 128\pi$.

is related to how the particles diffuse along the channels of the web. The analogy with a random walk makes it a comparatively simple matter to write a kinetic equation for the case of trivial resonances ($q = 3, 4, 6$). This situation is different for nontrivial resonances, in which case the structure of the web is very complex. If K_{II} is large, the particle diffusion can be described in the customary way by means of a Fokker-Planck-Kolmogorov equation.[5]

We go back to our original Hamiltonian, (3.3), and introduce some action-angle variables:

$$I = \dot{x}^2 + \omega_0^2 x^2, \quad \varphi = \operatorname{arctg} \frac{\omega_0 x}{\dot{x}}. \tag{3.26}$$

The quantity I is, within a constant factor, the energy of the particle (or oscillator). For small perturbations ε the changes in the energy upon each kick can be relatively small; i.e.,

$$| \Delta I | = | I_{n+1} - I_n | \ll I_n. \tag{3.27}$$

Inequality (3.27), however, may be compatible with the condition [see (3.10)]

$$K_H = \varepsilon \omega_0 T_0 \gg 1 \tag{3.28}$$

because of the large factor $\omega_0 T_0$ in it. Accordingly, there is a rapid mixing in the phase φ by virtue of (3.28). Condition (3.27) means that there is a slow diffusion change in the action. If $F(I, t)$ is the distribution function with respect to the action, the corresponding diffusion equation is

$$\frac{\partial F}{\partial t} = \frac{1}{2} \frac{\partial}{\partial I} D(I) \frac{\partial F}{\partial I}, \tag{3.29}$$

where the diffusion coefficient is

$$D(I) = \frac{1}{T} \ll (\Delta I)^2 \gg, \tag{3.30}$$

and $\ll \ldots \gg$ means an average over the phases.

From mapping T in (3.6) and definitions (3.26) we find

$$\Delta I = 2\varepsilon \frac{\omega_0^2}{k} T_0 I^{1/2} \sin \varphi \cdot \sin (k\rho \cos \varphi) + \left(\varepsilon \frac{\omega_0^2}{k} T_0\right)^2 \sin^2 (k\rho \cos \varphi), \quad \rho = \frac{\dot{x}}{\omega_0}. \tag{3.31}$$

Substituting (3.31) into (3.30), and carrying out some simple calculations, we find

$$D = \omega_0^2 K_H^2 \frac{I}{k^2 T_0} \left[1 - \frac{1}{k\rho} J_1 (2k\rho)\right], \tag{3.32}$$

where J_1 is a Bessel function. For motion in a magnetic field, ρ would have the meaning of a Larmor radius. If $k\rho > 1$ (weak magnetic fields), the diffusion coefficient D contains an oscillating factor. If $k\rho \gg 1$, then we have

$$D = \varepsilon^2 \frac{\omega_0^4}{k^2} T_0 I, \tag{3.33}$$

and the average energy of the particle increases in proportion to the time:

$$\langle I \rangle = Dt + I_0.$$

FIG. 11. The mapping point generates a diffusion fractal tree in the phase plane in the case of strong chaos, which preserves a q-fold symmetry. $q = 5$, $K_{II} = 20$, size of square $4 \cdot 10^3 \pi$, time of $4 \cdot 10^4$ mapping steps.

If the resonance condition $\omega_0 T_0 = 2\pi p/q$ holds, the overall picture of the diffusion will retain a q-fold symmetry, although the web is disrupted at $K_H \gg 1$ (Fig. 11). A fractal tree forms in the phase plane. The various forces acting in the equations of motion result in an unusual clustering of the diffusion. At large wave amplitudes (large values of K_H), a particle moves rapidly in the radial direction, forming q diffuse rays of irregular shape. The spreading of the rays in the azimuthal direction occurs comparatively slowly. Accordingly, if we adopt an initial condition such that the diffusion occurs primarily along other radii then the new fractal tree (cluster) will undergo no or almost no intersections with the preceding tree for a very long time. In this sense the phase plane is "clustered," i.e., broken up somewhat arbitrarily into certain fractal regions of diffusion, which overlap each other slightly.[25]

4. STRUCTURAL PROPERTIES OF A WEB

4.1. Which structures are possible?

When we attempt to learn why snowflakes have a hexagonal rather than, say, pentagonal shape, we find that we need to carry out a thorough study of the subtle geometric properties of objects produced by nature. Is it true that the laws of geometry forbid certain shapes for physical objects? In one form or another, questions of this sort date back to antiquity, and the use of symmetry laws in physics has become a completely customary method of analysis. Crystal physics is apparently a field in which the use of geometric ideas is particularly graphic. Orthodox crystallography is based on the representation of periodically repeating structures which fill a space or plane. More formally, a packing of one or several structural cells having translational symmetry with respect to displacement by a certain vector occurs in crystals. In such cases one speaks of the existence of a long-range order in crystals. In addition to translational symmetry there can simultaneously be a rotational symmetry through angles[23]

$$\alpha_q = \frac{2\pi}{q} \qquad (q = 3,\ 4,\ 6) \tag{4.1}$$

[conditions (4.1) are the same as those in the case of a web with trivial resonances]. The problem of realizing various types of crystal lattices is related in an obvious way to the problem of mosaics or tilings of a space or plane with a given type of symmetry. This problem belongs to the field of geometry, and it has been the subject of extensive research (see Refs. 26–29, 77, and 80). Although we can assign a fairly arbitrary shape to an individual cell, as can be seen from the inventive pictures of the Danish artist Escher,[30] we can use them to pave a plane only in a completely definite number of ways if we wish to preserve long-range order in the process.

In the long list of studies of tilings, packings, mosaics, ornaments, crystallography, etc., the number 5 always seems to occupy a special place. Attempts to learn to what extent a regular pentagon can be incorporated in tilings can be found even in the studies by Kepler and Dürer. While we find numerous Islamic ornaments which contain regular pentagons and decagons, we simultaneously find many assertions in the specialized literature that crystals with a fivefold symmetry axis cannot exist.

The concept of order is presently evolving. To a large extent, we can attribute these changes to progress in research on nonlinear dynamics, where a given system may execute either a regular or a chaotic motion, depending on the values of its parameters. Accordingly, a given algorithm for distributing atoms in a row (for example) can generate either a periodic arrangement of atoms or a stochastic arrangement.[31,32] The particular type of distribution of atoms may be determined exclusively by the values of a single parameter: the potential of an external field. There are also other distributions of atoms, which are in a sense intermediate between regular and chaotic distributions. In particular, the so-called incommensurate phases[33] fall in this category.

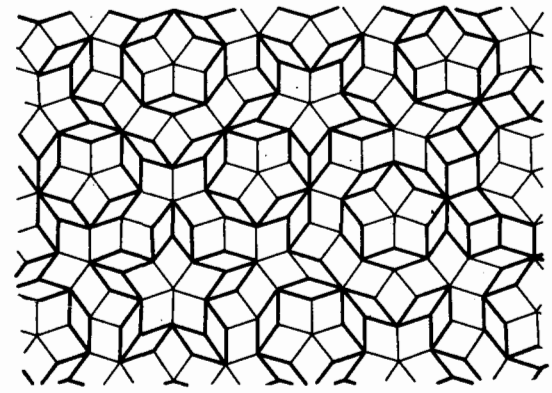

FIG. 12. Example of a Penrose parquet.

For some time now, crystallography has seen attempts to break away from the orthodox views of just what a crystal should be. Schrödinger[34] was the first to offer a well-argued case for the need for such a reexamination. In order to explain the structure of a large molecule which constitutes a single gene, he introduced the concept of an aperiodic crystal, for which the genetic code serves as the algorithm which specifies the order in the arrangement of atoms and groups of atoms. Many attempts to expand the old order schemes were concentrated around a search for structures with fivefold symmetry.[35,36] A special role was played by Penrose's construction,[37] to which interest was attracted to a large extent by Gardner's paper.[38] Penrose's parquet is an example of a new type of ordered structures which have come to be called "quasicrystals." It can be made up of two types of rhombi[36] (Fig. 12) and in this case has a symmetry axis.

The first quasicrystal with fivefold symmetry was discovered by Schectman *et al.*[39] in some experiments carried out for the purpose, involving a rapid cooling of an Al–Mn alloy. X-ray diffraction patterns revealed a sharp (not diffuse) system of spots which was evidence of the existence of a fivefold symmetry and a long-range order. The problem of the properties of quasicrystals has now been studied in many places (see the materials of a working conference on aperiodic crystals[40]). Here we will discuss only certain specific aspects of these problems which (first) are directly related to the properties of a uniform stochastic web and (second) are related to the plane case.

4.2. The projection method and dynamic generation of structures

One of the first methods for producing quasicrystal structures was based on the projection of close-packed N-dimensional cubes from an N-dimensional space onto some D-dimensional ($D < N$) space. With $D = 2$ and $N = 5$, the

result was a Penrose parquet. The projection technique, which was begun in Ref. 41, was developed systematically in Refs. 42–48. Let us outline its basic idea.

We consider a system of orthogonal unit vectors $\{\mathbf{e}_j\}$ ($j = 1, \ldots, q$) which emerge from a common point. With each vector $\mathbf{e}_j$ we associate an unbounded system of equidistant parallel $(q-1)$-dimensional hypersurfaces in a q-dimensional space. This family of hypersurface is called a "grid." A set of q grids forms a multigrid of order q. The intersections of hypersurfaces form a q-dimensional generalization of a square lattice. The projection of a multigrid onto a D-dimensional space generates a tiling or mosaic. It is in this manner that a Penrose parquet arises, and it can be proved that this parquet has no "holes" or intersecting rhombi.[41]

In a more general case, a grid can be constructed in a more complex way (e.g., with certain gaps), but it is clear that the projection operation is linear. This important conclusion means that in the course of the projection regular multigrids create a complex parquet of ordered structures which definitely have a long-range order. As we will see, however, the long-range order in this case is due not to a periodicity but to a near-periodicity (a finite number of incommensurate periods) or a conditional periodicity (an infinite number of incommensurate periods) of the structures.

There are further generalizations of the projection idea for generating aperiodic structures. For example, the system of vectors $\{\mathbf{e}_j\}$ can form an arbitrary (irregular) star, and a family of straight lines can be curved in a certain way.[78]

The most important property of a Penrose parquet and of other tilings which arise during the projection of lattices is a local isomorphism[48,78]: If we focus on any finite part of a parquet, we will find it again an infinite number of times in the entire parquet.

The Fourier transform of a Penrose parquet[36] is the same as the x-ray diffraction patterns of real quasicrystals,[39,40] which are also called "shectmanites." Nevertheless, the relationship between quasicrystals and the structures generated by a projection method is still a formal one and does not follow from first principles. A particular consequence of this circumstance is that it is not possible to specify the positions of atoms in a real quasicrystal lattice.[49]

Another approach to structures of the quasicrystal type starts from Landau's theory, according to which, for example, the electron density $\eta(r)$ must have the same symmetry as the crystal lattice. The density can accordingly be written as the expansion[44,49–53]

$$\eta(\mathbf{r}) = \sum_{\mathbf{k}} \eta_{\mathbf{k}} e^{i\mathbf{k}\mathbf{r}}, \tag{4.2}$$

where the vectors $\mathbf{k}$ form a reciprocal-lattice basis. In the plane case there are five such fundamental vectors k_i ($i = 1, \ldots, 5$), and we find an expression like (3.14), (3.17) for H_q, although with a different content.

A third approach to the analysis of quasicrystal symmetry starts from the use of a real dynamic model which generates this symmetry.[5,21,25,54] The symmetry generator is a mapping with a twisting, $\hat{M}_q$ [see (3.9)], under resonance conditions (3.11):

$$\begin{aligned} &\hat{M}_q: \\ &\bar{u} = (u + K_H \sin v)\cos\frac{2\pi}{q} + v\sin\frac{2\pi}{q}, \\ &\bar{v} = -(u + K_H \sin v)\sin\frac{2\pi}{q} + v\cos\frac{2\pi}{q}. \end{aligned} \tag{4.3}$$

The mapping $\hat{M}_q$ acts in the two-dimensional space (u, v), and at small values of K_H its disrupted separatrix network (stochastic web) forms an invariant tiling of a plane with a q-fold quasicrystal symmetry. In accordance with (3.14) and (3.15), we write the average Hamiltonian H_q for mapping (4.3) in the following form (within a constant factor):

$$\begin{aligned} &\bar{H}_q = -\sum_{j=1}^{q} \cos(\mathbf{e}_j\mathbf{R}); \\ &\mathbf{R} = (v,\ u), \quad \mathbf{e}_j = \left(\cos\frac{2\pi}{q}j,\ \sin\frac{2\pi}{q}j\right). \end{aligned} \tag{4.4}$$

It is not difficult to establish an analogy between (4.4) and (4.2), but we now have some additional information which allows us not only to treat $\bar{H}_q$ as a Hamiltonian but also to study a perturbation of it by the methods of Hamiltonian mechanics.

Arnol'd[83] has recently mentioned yet another approach to the problem of the symmetry of partitionings, in which a relationship is established among quasicrystal symmetry, Markov partitionings, and the theory of singularities.

4.3. Smoothed structures

The concept of the symmetry of the tilings which are generated by expression (4.4) is based on the structure of the separatrices and the arrangement of the singular points which are generated by the Hamiltonian $\bar{H}_q$. Let us consider, for example, the contour lines $\bar{H}_q = E$. This is a family of a large number of closed invariant curves of various sizes and shapes. The structures which are generated by the phase portrait of $\bar{H}_q$ will be called "smoothed with respect to the stochastic web," which contains considerably more small details. Despite this simplification in the research on webs, the problem of the phase portrait of an integrable dynamic system with Hamiltonian $\bar{H}_q$ remains a complicated one.

Figure 13 shows the distribution of the number of elliptical points ρ_e for various energies in the cases of fivefold and sevenfold symmetry (the normalization of ρ_e is arbitrary).[54] The region of values $E = \bar{H}_q > 0$ corresponds to stable points (the bottom of the potential relief), while the region $E = \bar{H}_q < 0$ corresponds to unstable points (the top of the potential relief). Figure 14 shows a corresponding distribution of hyperbolic points ρ_h. In contrast with the case of trivial resonances with $q = 3$, 4, and 6 (i.e., the cases of ordinary crystal lattices), where the singular points of the energy relief lie on surfaces with strictly fixed energy values, there is now a spread in the distribution of these points. A web of this sort is usually characteristic of disordered systems. In the case at hand we are seeing it in a system with a long-range order; this fact is somewhat surprising.

It is now clear that there are very many separatrices and that they lie at different energy levels. Some of them have parts which run close to each other. Even a very small perturbation will disrupt the separatrices. In their place, stochastic layers of finite thickness will form. The narrow gaps between close-lying sections of separatrices grow and form a large network. This network is the basic stochastic web of the generator of structures in (4.3). We have described the basic element of coupling between the original dynamic system, specified by Eqs. (4.3), and the average system with a smoothed structure, defined in (4.4). If we wish to observe this smoothed structure, we should proceed in the following

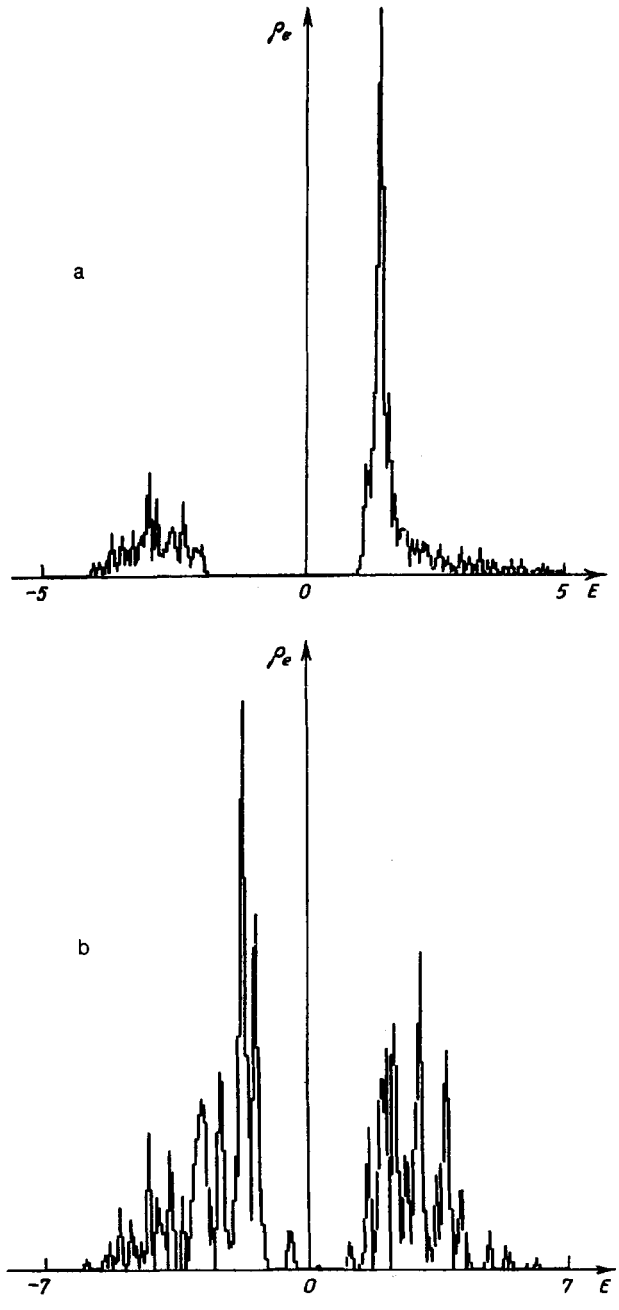

FIG. 13. Energy distribution of elliptical points. a—$q = 5$; b—$q = 7$. The points at $\overline{H}_q > 0$ are stable, and those at $\overline{H}_q < 0$ are unstable.

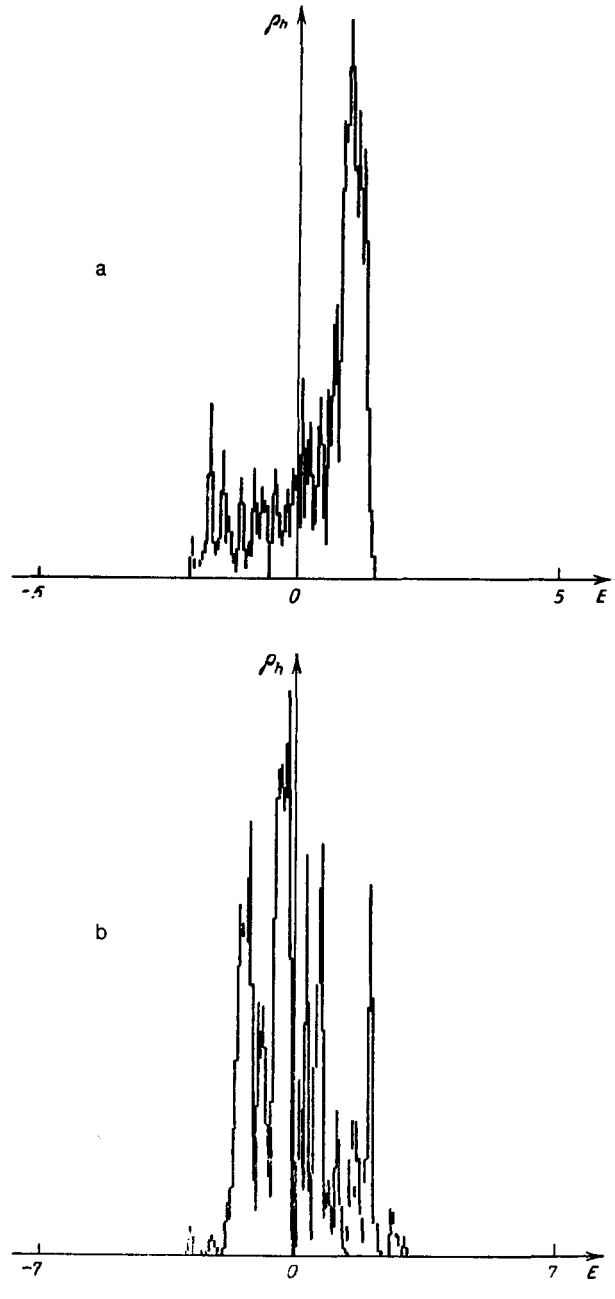

FIG. 14. Energy distribution of hyperbolic points. a—$q = 5$; b—$q = 7$ (Ref. 54).

way: We consider a narrow energy layer ΔE which lies near that energy E_c which corresponds to the maximum of the hyperbolic points ($E_c = 1$ for $q = 5$ and $E_c \approx -1$ for $q = 7$). The (u, v) points which lie on the paths of the system with the Hamiltonian $\overline{H}_q$ and with an energy $E \in E_c \pm \Delta E/2$ determine the smoothed equivalent of the stochastic web of the generator $\hat{M}_q$. We call the set of these points the "energy relief of the structure." Figure 15 (Ref. 21) shows examples of energy reliefs for the cases $q = 5, 7$; Fig. 16 shows examples for $q = 8, 12$. These reliefs constitute a simplified version of the stochastic web shown in Figs. 9 and 10. A quasicrystal with a 12-fold symmetry was observed in Ref. 55, and quasicrystals with eightfold symmetry were observed in Ref. 81. One might imagine that the function $\overline{H}_q(u, v)$ determines a two-dimensional potential relief in the (u, v) plane. The atoms should then lie near stable elliptical points. If we retain only those points which lie near maxima of the ρ_e distribution in Fig. 13, we find, in the case $q = 5$, an example of a structure (Fig. 17)[54] which a two-dimensional quasicrystal might have. The large dark spots mean that the region where there might be an atom has a certain size. This circumstance is in turn a consequence of the flat bottom of the potential well. Figure 17 thus gives an idea of the structure of a plane quasicrystal film with a fivefold symmetry. The smoothed structures which are generated by the energy reliefs have a symmetry under rotation through an angle π/q if q is odd (Fig. 15) or through an angle of $2\pi/q$ if q is even (Fig. 17). On the contrary, the structures which are formed by the web always have a q-fold symmetry. Everywhere below we will be speaking in terms of a q-fold symmetry, hav-

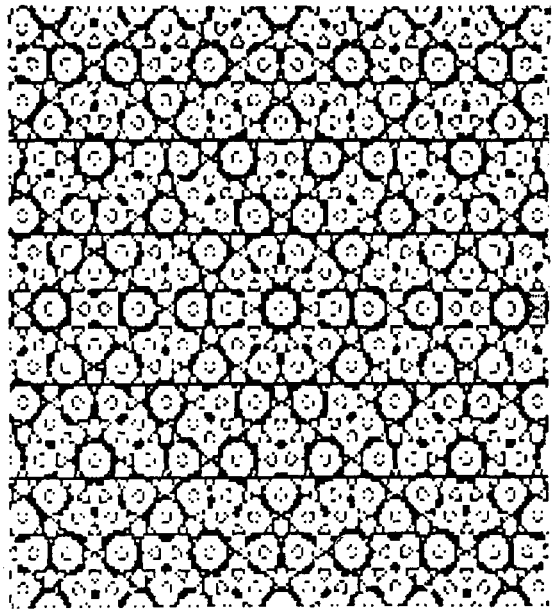

a

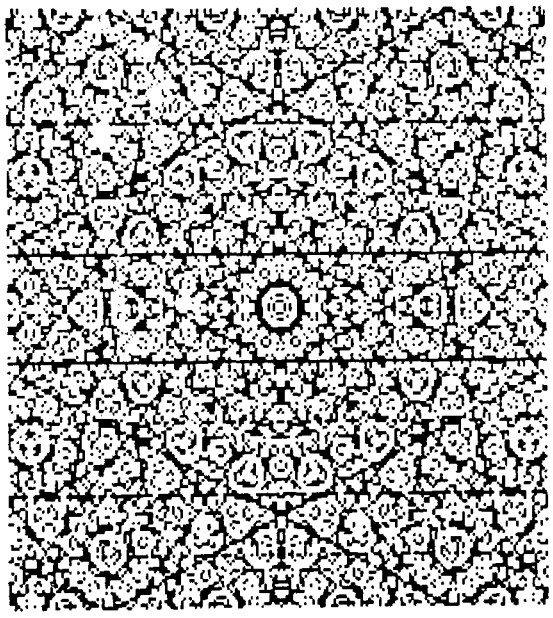

b

FIG. 15. Energy reliefs. a—$q = 5$, size of square $64\pi \times 64\pi$; b—$q = 7$, size of square $80\pi \times 80\pi$.

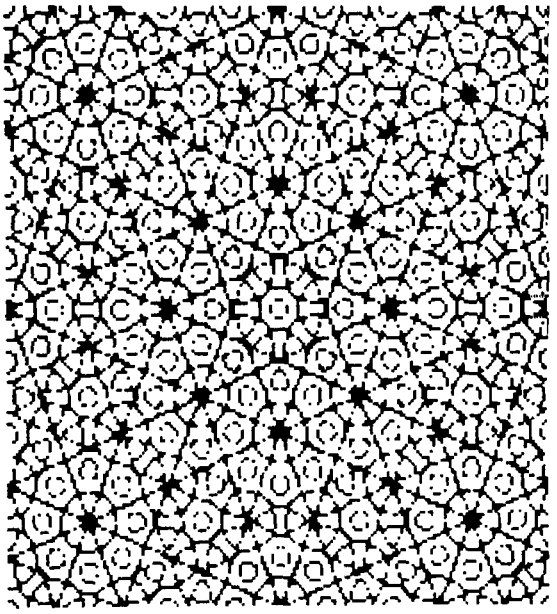

a

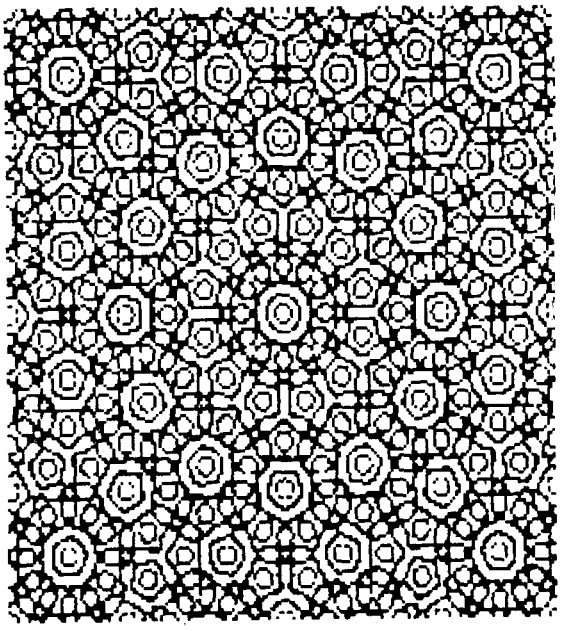

b

FIG. 16. Energy reliefs. a—$q = 8$, size of square $48\pi \times 48\pi$; b—$q = 12$, size of square $56\pi \times 56\pi$.

ing in mind the defining number q in the tiling generator (4.3) or in the average Hamiltonian (4.4).

Smoothed structures have a scale invariance, but this property has not been studied adequately.

4.4. Quasisymmetry, decoration, underlattices, and sublattices

As we have already mentioned, a stochastic web is fractal, so its detailed shape is very complicated. The more precisely we wish to determine the shape of its boundaries, the more complicated the pattern which is observed. This property is inherent in any stochastic layer. Consequently, we can hardly speak in terms of any point symmetry. The interaction of translational and rotational symmetries should disrupt both, even if the coupling constants K_H are small. Symmetric defects may be weak, however, so a symmetry will exist in some approximate and perhaps poorly defined sense. We understand at an intuitive level that a certain degree of coarsening of a web will make it more regular, i.e., more "symmetric." It is accordingly useful on occasion to move away from a determination of some "pure" symmetry and to use in its place a "quasisymmetry." This is the role which is played by the mapping $\hat{M}_q$, which may be thought of as a generator of tilings with a "quasisymmetry" of the "quasicrystal" type. In this sense the smoothed structures specified by Hamiltonian (4.4) are more "regular." When we go from a web to smoothed reliefs, there is some smoothing out of lines, and certain elements disappear. It can thus be assumed

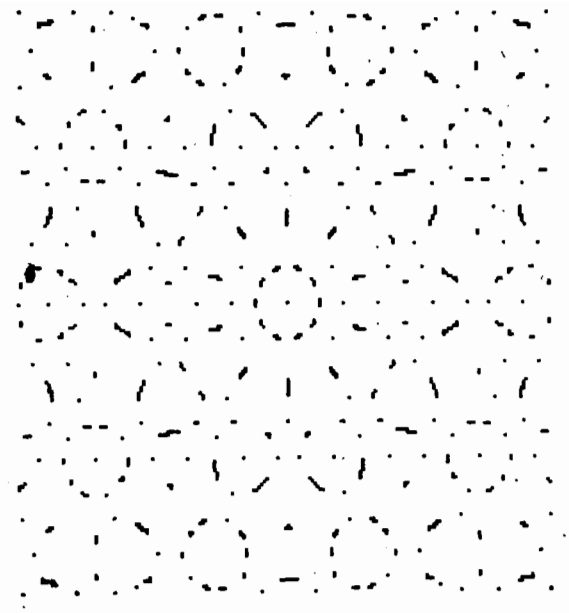

FIG. 17. Example of a plane fivefold quasicrystal lattice.[54] The dark spots correspond to the most probable regions for the localization of atoms. The size of the square is the same as in Fig. 14a.

that a relief is a certain decoration of a web.

In general, a set of different tilings can be constructed on the basis of a web or relief if we use some additional algorithm to connect the different points of the main figure. This operation is naturally called a "decoration." A Penrose parquet can be found easily as a decoration of the structure in Fig. 15a (Ref. 21). Correspondingly, we can generate a sevenfold mosaic (Fig. 18) as a decoration of the relief in Fig. 15b, by using simply three rhombi with acute angles $\pi/7$, $2\pi/7$, and $3\pi/7$. Parquets of the type in Fig. 12 or 18 can in turn be decorated, with the result that we obtain new tilings with the same symmetry.[51]

Certain decoration ideas are associated with the formation of stars of the type in Fig. 9b. Such stars are Koch-curve fractals, and their fractal dimensionality is $D = 1.44$ (Ref. 56).

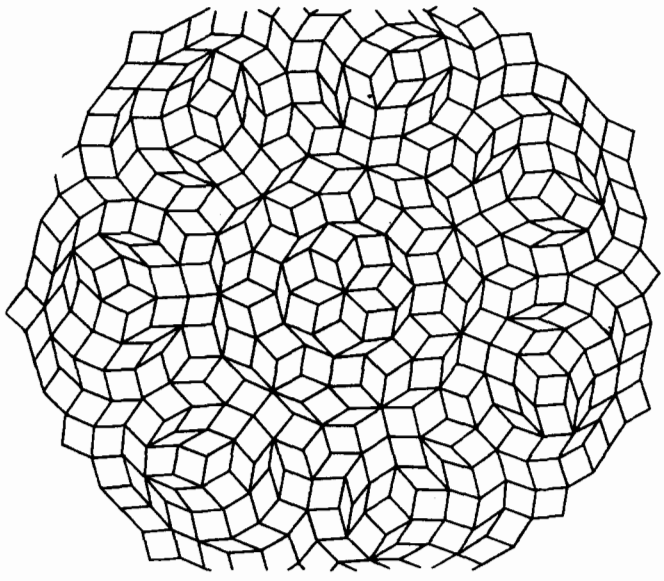

FIG. 18. Example of a sevenfold mosaic.

In the smoothed structures in Fig. 15 we can distinguish a system of straight lines which form a multigrid, i.e., a system of parallel straight lines which are rotated q times through an angle of $2\pi/q$. Let us consider, for example, the pentagrid in Fig. 15a. The system of straight lines in it has a different thickness, and the distance between any pair of adjacent straight lines is $a_n = a_0\tau_0^n$, where a_0 is the minimum distance, $\tau_0 = (1+\sqrt{5})/2 = 2\cos(\pi/5)$ is the golden section, and n is any integer. We define a filter process as follows: We shall delete, for example, all the straight lines in Fig. 15a except those which form a pentagrid with only two possible distances between neighboring parallel lines: a_n and a_{n-1} $(n \geqslant 1)$, where the number n is fixed. The pentagrid formed in this way is also called an "Ammann lattice." The coordinates x_m of the parallel lines in an Ammann lattice satisfy the simple rule[48]

$$x_m = m + \alpha + \frac{1}{\tau_0}\left[\frac{m}{\tau_0} + \beta\right],$$

where m is an integer, α and β are constants, and [. . .] means the greatest integer.

Another way to depict the sequence of alternations of two distances a_0 and b_0 between lines in an Ammann lattice involves the use of the mapping[48]

$$\hat{T}_5 = \begin{pmatrix} 1 & 1 \\ 1 & 0 \end{pmatrix},$$

which acts on the column vector (a_0, b_0). It generates

$$a_1 = a_0 + b_0, \quad b_1 = a_0,$$
$$a_2 = a_1 + b_1 = a_0 + b_0 + a_0, \quad b_2 = a_1 = a_0 + b_0 \ldots .$$

The sequence $\lim_{n\to\infty} a_n$, in which the order of alternation of lines a_0 and b_0 is fixed, is called a "Fibonacci sequence." It determines an Ammann lattice in the case $q = 5$.

With $q = 7$, the operator $\hat{T}_7$ is nonlinear, and the sequence of lines in the lattice is determined not by a single number, as in the $q = 5$ case, but by two numbers, e.g., $\tau_1 = \cos(\pi/7)$ and $\tau_2 = \cos(2\pi/7)$.

The lattices generated by the filtering are naturally called "underlattices." They also represent a certain primitive type of decoration. The very fact that a filtering process exists reflects the property of scale invariance of the original structures.

One important property of quasicrystal symmetry is the possibility of distinguishing sublattices as one does in ordinary crystals. We denote by $\mathscr{H}_q[f(\theta)]$ the generalized Hamiltonian which generates a quasicrystal tiling of a plane:

$$\mathscr{H}_q[f(\theta)] = \sum_{j=1}^{q} f(\theta_j), \tag{4.5}$$

where f is an arbitrary function, and

$$\theta_j = \mathbf{e}_j\mathbf{R}. \tag{4.6}$$

We then have the following identity:

$$\mathscr{H}_{nq}[f(\theta)] = \sum_{l=0}^{n-1} \mathscr{H}_q\left[f\left(\theta + \frac{2\pi}{n}l\right)\right], \tag{4.7}$$

where n is an integer. We thus see that from a q-fold lattice we can, through an n-fold rotation through an angle of $2\pi/n$, form a q'-fold lattice where $q' = nq$. The Hamiltonian of the resulting lattice is a simple superposition of the Hamilto-

nians of the sublattices. This property is important for constructing models which contain an interaction of sublattices.

4.5. Fourier analysis of structures

Fourier analysis is an important tool for studying the structural properties of a stochastic web and of reliefs in the phase plane. Furthermore, x-ray analysis of real crystals reveals information about their symmetry properties. The picture of the Fourier spectrum of a structure in a case of a fivefold symmetry (a Penrose tiling) appeared in Ref. 35 before the corresponding pattern was found experimentally.[39] A comparison of the Fourier spectra of structures formed by the energy reliefs of a Hamiltonian $\overline{H}_5$ with experimental spectra was carried out in Ref. 79. All these results support the suggestion that a Fourier spectrum with the pattern of a tiling of a plane conveys quite well the symmetry properties of the tiling, although it does not allow one to reconstruct the tiling unambiguously.

We denote by S_Γ the set of points which belong to some figure (or structure) in a phase plane of size Γ. We also assume

$$\delta(\mathbf{R}-\mathbf{R}_s)=1, \quad s\in S_\Gamma,$$
$$=0, \quad s\notin S_\Gamma,$$

where $\mathbf{R}$ is the vector of an arbitrary point in the Γ plane, and $\mathbf{R}_s$ is the vector of a fixed point s. The Fourier transform of the structure is then given by

$$S(\mathbf{k})=\lim_{\Gamma\to\infty}\frac{1}{(2\pi)^2}\int e^{i\mathbf{k}\mathbf{R}}\delta(\mathbf{R}-\mathbf{R}_s)\,d\mathbf{R}. \tag{4.8}$$

In reality, we are always dealing with a finite region Γ. We thus have some additional boundary effects in the form of $S(\mathbf{k})$. For periodic structures S, they can sometimes be distinguished easily. In the case of aperiodic tilings of a plane, however, it is not possible to distinguish a "single crystal."

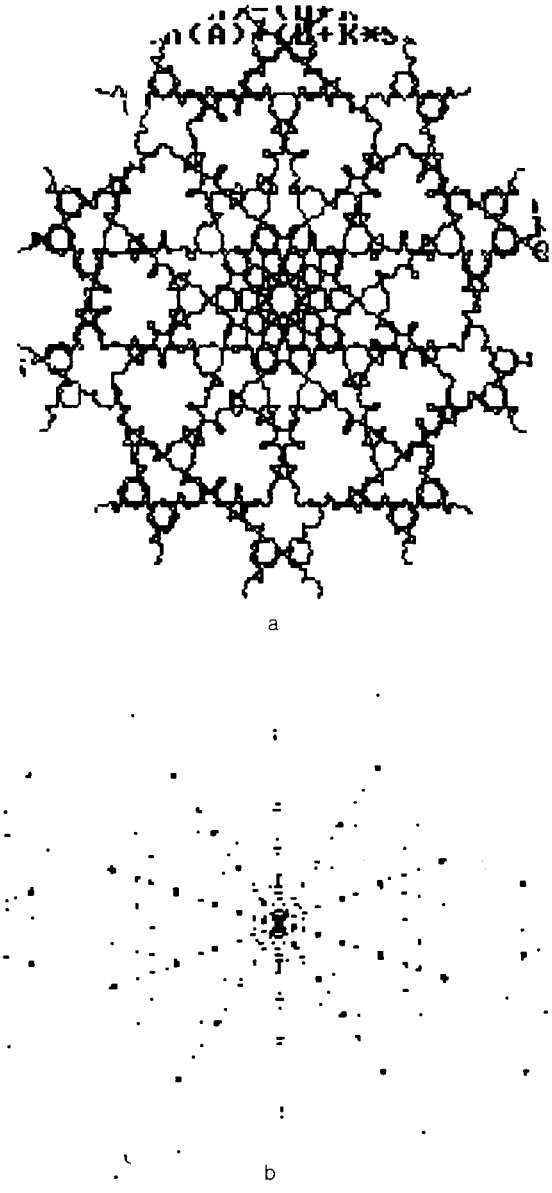

FIG. 19. a—Element of a web for $q = 5$ (the radius of the circle is 50π); b—its Fourier transform.

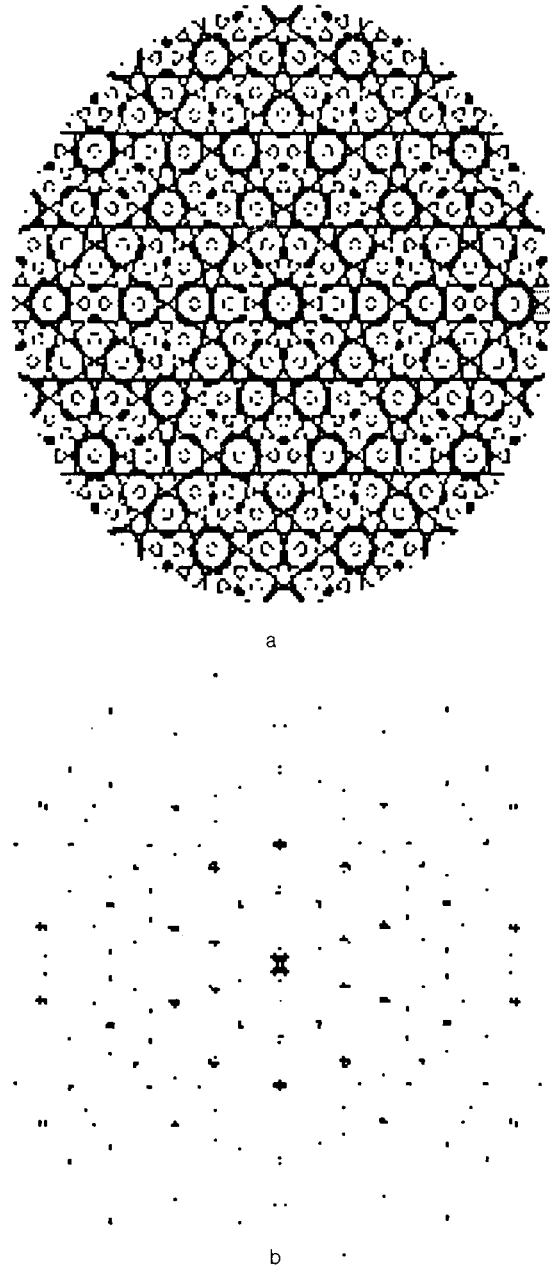

FIG. 20. a—Element of an energy relief for $q = 5$ (the radius of the circle is 32π); b—its Fourier transform.

In such a case, however, one can use the property of rotational symmetry and the property of simiarity of structures of the quasicrystal type.

Figures 19b and 20b show Fourier spectra for, respectively, the stochastic web generated by $\hat{M}_5$ and the energy relief of the same smoothed structure generated by $\overline{H}_5$. The region Γ was chosen to be a circle; this choice gives us a fairly good approximation of the web in Fig. 19a. The patterns in Figs. 19b and 20b are similar. This is a very important consequence, since it confirms that it is possible to introduce a symmetry analysis of infinite webs of dynamic systems, as is done for crystals or quasicrystals. A corresponding equivalence can be seen in the $q = 7$ case from Figs. 21 and 22.

We now choose two regions of the relief: one in the central part of the structure, with $q = 11$ (Fig. 23a), and the other somewhere else in the plane, far from the center (Fig. 24a). From the external appearance of the latter we can say nothing about either the symmetry of this region or the degree of order of the entire structure of which it is part. However, the corresponding Fourier spectrum of this region (Fig. 24b) is essentially identical to the Fourier spectrum of the central region (Fig. 23b). This property of quasicrystal structures reflects a new idea about possible types of order with rotational symmetry.

4.6. Singularities in the energy dependence of the phase volume (Van Hove singularities)

The Hamiltonian of the smoothed structures, $\overline{H}_q$, can be used to analyze certain subtle structural characteristics of a stochastic web. Among these characteristics are Van Hove singularities, which are associated with the existence of elliptical and hyperbolic singular points in phase space.[22] Let us assume, for example, that a system with a single degree of freedom executes a finite motion with an energy E. The

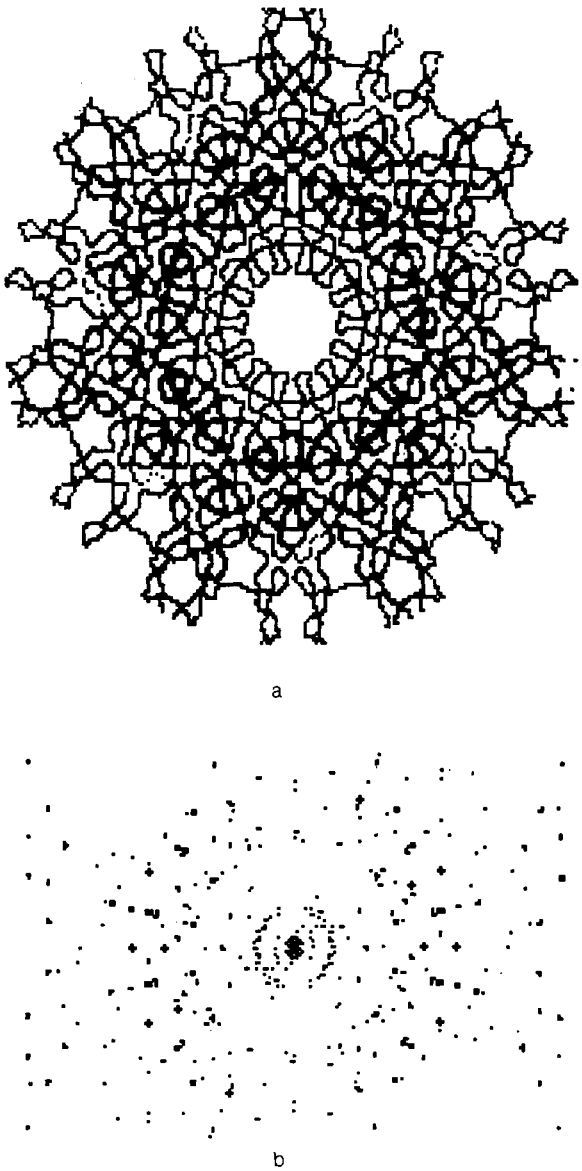

FIG. 21. a—Element of a web for $q = 7$ (the radius of the circle is 24π); b—its Fourier transform.

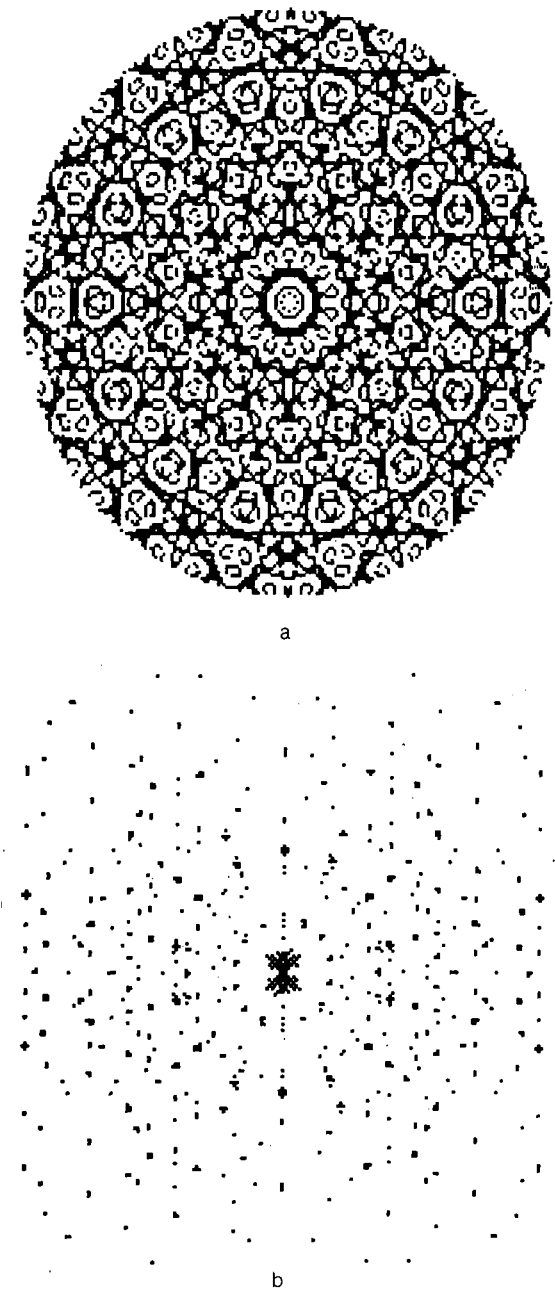

FIG. 22. a—Element of the energy relief for $q = 7$ (a circle of radius 32π); b—its Fourier transform.

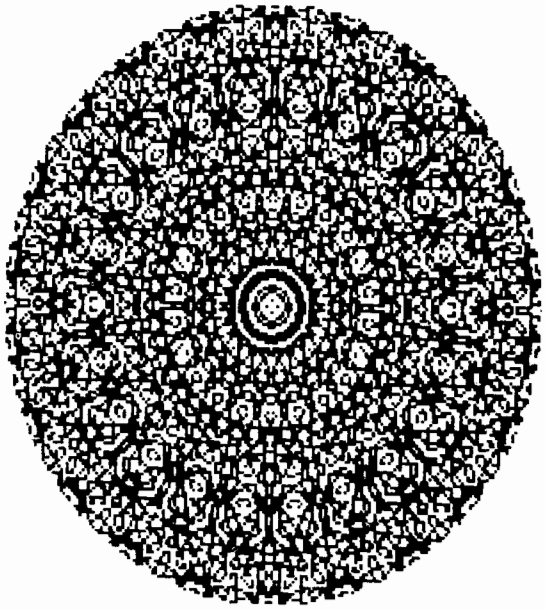

a

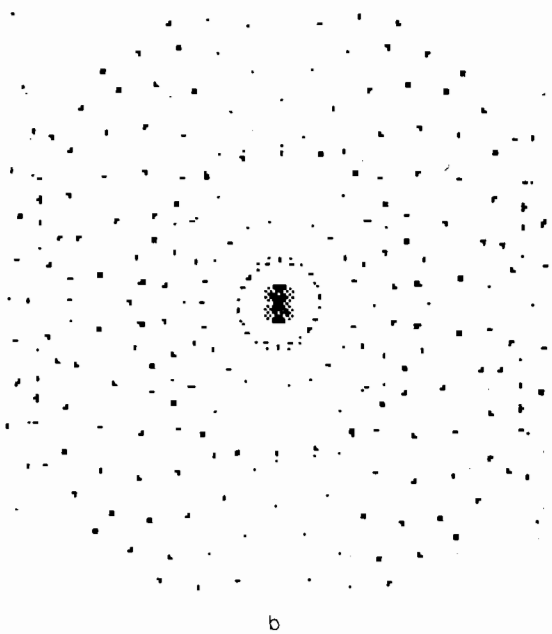

b

FIG. 23. a—Central part of the relief with $q = 11$; b—its Fourier transform.

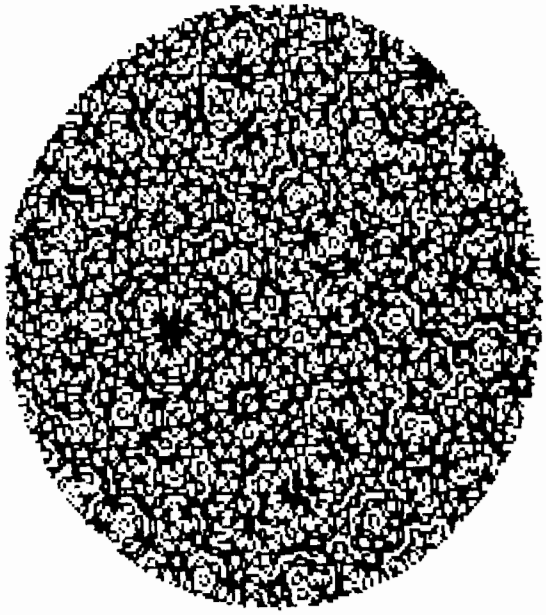

a

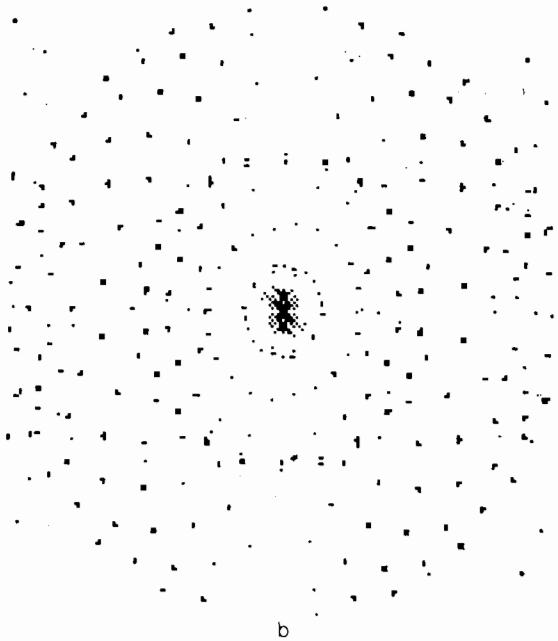

b

FIG. 24. a—Noncentral part of the relief with $q = 11$; b—its Fourier spectrum.

phase volume $\Gamma(E)$ bounded by the hypersurface (in this case, a curve)

$$H(p, x) = E \tag{4.9}$$

is

$$\Gamma(E) = \int\limits_{H \leqslant E} \mathrm{d}p\,\mathrm{d}x = \oint p(E, q)\,\mathrm{d}q, \tag{4.10}$$

where the integration contour in the latter integral is a path on hypersurface (4.9). The number of states with energies $\leqslant E$ is known[22] to be equal, apart from a constant, to the phase volume $\Gamma(E)$, and the state density is

$$\rho(E) = \mathrm{const} \cdot \frac{\mathrm{d}\Gamma(E)}{\mathrm{d}E} = \mathrm{const} \cdot \oint \frac{\partial p}{\partial E}\,\mathrm{d}q. \tag{4.11}$$

For a single degree of freedom we have

$$\rho(E) = \mathrm{const} \cdot T(E), \tag{4.12}$$

where $T(E)$ is the period of the oscillation of a particle with an energy E. It is then immediately clear that the singular points of the state density are singular points of the oscillation period in this case. For a single degree of freedom near the elliptical point there is a discontinuity of the nature of a jump in the function, associated with the boundary of the region of permissible values of the energy; near the hyperbolic point there is a logarithmic singularity associated with a divergence of the oscillation period at the separatrix.

For the dynamic systems which we are examining in this paper [see, for example, Hamiltonian (4.4)] the motion is organized in a more complex way. Corresponding to hypersurface (4.9) is not a single closed loop but an infinite

number of closed loops, which lie in the $H = E$ plane and form a corresponding structure in it. Accordingly, expression (4.10) for the phase volume is replaced by

$$\Gamma(E) = \sum \oint p(E, q)\, dq, \tag{4.13}$$

where the sum is over all closed phase loops. Expression (4.13) diverges. We will thus use a different representation for the state density. We consider the rectangle ($|p| < P_0$, $|q| < Q_0$). In place of (4.11) we define

$$\rho_0(E) = \lim_{P_0, Q_0 \to \infty} \frac{1}{\Gamma_0} \sum \oint \frac{\partial p(E, q)}{\partial E}\, dq, \tag{4.14}$$

where $\Gamma_0 = P_0 Q_0$, and ρ_0 is the normalized state density. We expect that the similarity property of the phase portrait generated by the Hamiltonian of the smoothed structures, $\overline{H}_q$ [see (4.4)], will lead to the existence of a limit in (4.14). In the cases $q = 3$, 4, and 6 (the symmetries of crystals) it is sufficient to consider only a single cell of the structure in the calculation of ρ_0, since the structure is periodic. In the case of quasicrystal symmetry, however, the comment regarding the possible use of expression (4.14) becomes nontrivial.

The main property of the quantity $\rho_0(E)$ is that it can be found from the classical (i.e., not quantum-mechanical) expressions, as we can see, in particular, from (4.12). We will first write some simple analytic expressions for $q = 4$ and $q = 3$.

For $q = 4$ we write

$$\mathcal{H} = \cos p + \cos x. \tag{4.15}$$

Hence

$$\rho_0(E) = \oint \frac{dx}{[1 - (E - \cos x)^2]^{1/2}} = 4K\left(\left(1 - \frac{E^2}{4}\right)^{1/2}\right), \tag{4.16}$$

where K is the complete elliptic integral of the first kind. As $|E| \to 0$ and $|E| \to 2$, i.e., near hyperbolic and elliptical points, respectively, we find from (4.16)

$$\begin{aligned} \rho_0(E) &= 4 \ln \frac{8}{|E|}, \quad |E| \to 0, \\ &= 2\pi, \qquad\quad |E| \to 2. \end{aligned} \tag{4.17}$$

Figure 25b shows the form of $\rho_0(E)$ for $q = 4$, illustrating the numerical method used.

For $q = 3$ we write

$$\mathcal{H} = \cos x + \cos\left(\frac{x}{2} + \frac{\sqrt{3}}{2} p\right) + \cos\left(\frac{x}{2} - \frac{\sqrt{3}}{2} p\right). \tag{4.18}$$

From (4.18) and (4.14) we find

$$\rho_0(E) = \frac{2}{\sqrt{3}} \oint dx\, [2(1 + \cos x) - (E - \cos x)^2]^{-1/2}. \tag{4.19}$$

There exist two energy intervals with different expressions for $\rho_0(E)$.

In the interval $-1 < E \leqslant 3$ we find from (4.19)

$$\rho_0(E) = \frac{8}{\sqrt{3}} (2E + 3)^{-1/4} K\left(\frac{\{[1 + (2E + 3)^{1/2}]^2 - (1 + E)^2\}^{1/2}}{2(2E + 3)^{1/4}}\right). \tag{4.20}$$

Hence

$$\begin{aligned} \rho_0(E) &= \frac{4\pi}{3}, \qquad\qquad E \to 3, \\ &= 4\sqrt{3} \ln \frac{1}{|E + 1|}, \quad E \to -1. \end{aligned} \tag{4.21}$$

In the interval $-3/2 \leqslant E < -1$ we find from (4.19)

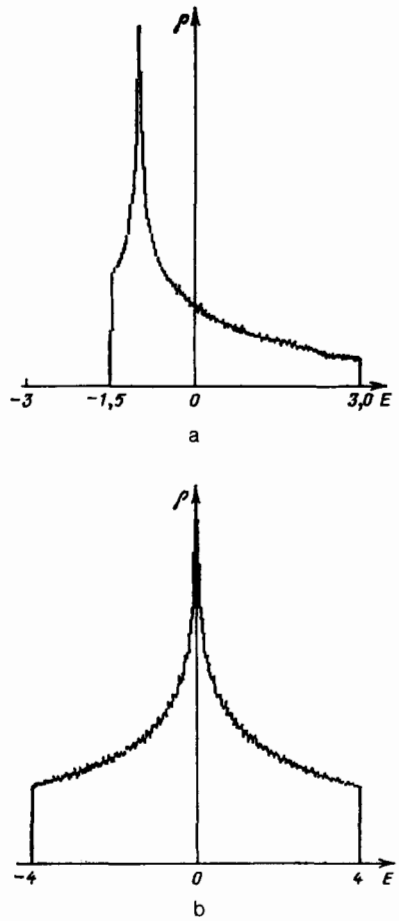

FIG. 25. State density and Van Hove singularities in the case of crystalline symmetry. a—$q = 3$; b—$q = 4$ (the absolute values of ρ are in arbitrary units).

$$\rho_0(E) = \frac{16}{\sqrt{3}} \{[1 + (2E + 3)^{1/2}]^2 - (1 + E)^2\}^{-1/2} \times K\left(\frac{2(2E + 3)^{1/4}}{\{[1 + (2E + 3)^{1/2}]^2 - (1 + E)^2\}^{1/2}}\right). \tag{4.22}$$

Hence

$$\begin{aligned} \rho_0(E) &= \frac{16\pi}{3} = 4\rho_0(3), \qquad E \to -\frac{3}{2}, \\ &= 4\sqrt{3} \ln \frac{1}{|E + 1|}, \quad E \to -1. \end{aligned} \tag{4.23}$$

Values $E < -3/2$ are not possible for Hamiltonian (4.18). The corresponding form of $\rho_0(E)$ found numerically is shown in Fig. 25a.

In cases of quasicrystal symmetry ($q = 5$, 7, 8, etc.), there are no analytic expressions for $\rho_0(E)$. A numerical analysis[54] leads to the distributions $\rho_0(E)$ shown in Fig. 26. We see that for those values of E for which the distributions of the elliptical and hyperbolic points have maxima (cf. Figs. 13 and 14) there are clear traces of Van Hove singularities. Now, however, they are smoothed out to a great extent, and the entire pattern is more reminiscent of a liquid than a crystal. Beginning at $q = 7$ the distribution $\rho_0(E)$ is essentially the same as that in the cases with $q > 7$. The smoothing of the singularities in the case of a quasicrystal symmetry can be classified as a distinctive property of this symmetry. Various decoration methods can significantly deplete the structure

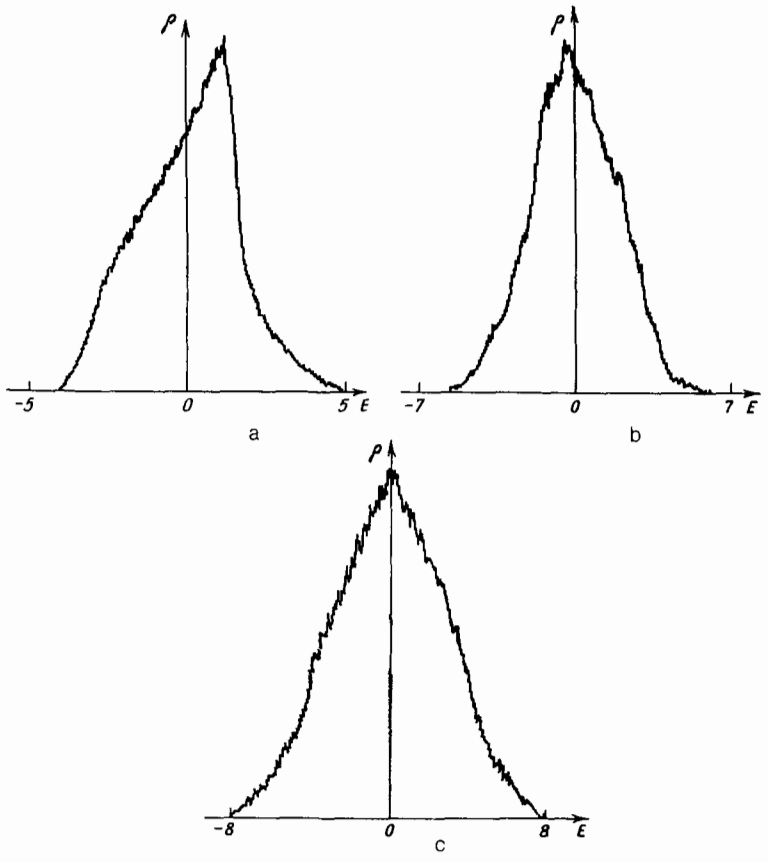

FIG. 26. State density and Van Hove singularities in cases of quasicrystal symmetry. a—$q = 5$; b—$q = 7$; c—$q = 8$.

and intensify the manifestation of Van Hove singularities. This is the situation, for example, with a Penrose parquet.[57]

4.7. Comment regarding the spectral properties of structures

Until recently, our picture of the nature of possible structures was comparatively simple. It included the concepts of crystals and liquids; the various disordered media were usually included with the liquids. The appearance of a quasicrystal symmetry requires clearer and sharper definitions. More precisely, it is necessary to build a more definite meaning into what we should call an "ordered structure" and just what we should call a "disordered" or "amorphous" structure. The situation is that quasicrystal structures should have been classified as structures with a long-range order, as can be seen, for example, from their x-ray diffraction patterns or Fourier spectra. However, the form of the state density $\rho_0(E)$ with smoothed Van Hove singularities is evidence more of a disordered entity than of a crystal.

Part of the reason for the paradoxes which arise is that the configuration of the structures in the quasicrystal case is specified by an algorithm which is more complicated than that in the crystalline case. We thus need to apply the more precise definitions regarding the concept of order to an algorithm which specifies the method for building a structure. Such definitions already exist in the theory of dynamic systems, and they can be used in describing the properties of structures.

Let us assume that the vector ξ specifies the position of some structural element, while the position of another element η is determined by some operator $\hat{T}$:

$$\eta = \hat{T}(\eta|\xi)\,\xi. \tag{4.24}$$

Equation (4.24) determines a dynamic system in the phase space (ξ) if all the structural elements ξ_n are numbered in some way. This is possible, since the set of these elements is countable. In the coordinate system which we have introduced we can thus write in place of (4.24)

$$\xi_{n+m} = \hat{T}_m(n)\,\xi_n. \tag{4.25}$$

The "spectrum" of dynamic system (4.25) is the quantity $\mathscr{R}(\mathbf{k})$, which is the Fourier transform of the correlation function $R(f, f \mid x)$:

$$\mathscr{R}(f,\ f|\mathbf{x}) = \int_{-\infty}^{+\infty} d\mathbf{k} e^{i\mathbf{k}\mathbf{x}} \mathscr{R}(\mathbf{k}),$$

$$\mathscr{R}(f,\ g|m) \equiv \int d\xi_n f(\xi_{n+m})\, g(\xi_n)$$

$$- \int d(\xi_{n+m})\, f(\xi_{n+m}) \int d\xi_n g(\xi_n), \tag{4.26}$$

where f and g are arbitrary integrable functions. The entire question about the nature of the structure now reduces to the form of the spectrum $\mathscr{R}(\mathbf{k})$.

If the mapping (4.25) determines only an ergodic "path," its spectrum $\mathscr{R}(\mathbf{k})$ is discrete:

$$\mathscr{R}(\mathbf{k}) = \sum_{\nu} \mathscr{R}_\nu \delta(\mathbf{k} - \mathbf{k}_\nu), \tag{4.27}$$

where the set of wave numbers k_ν determines possible periods of the structure. In the case of a periodic chain, for example, there is only a single value, k_0 (if we do not count possible values nk_0). For any Ammann quasicrystal lattice,

however, two values, k_1 and k_2, which are incommensurate appear.

Another possibility stems from the circumstance that the spectrum $\mathscr{R}(\mathbf{k})$ may be continuous. This case corresponds to the case of uncoupling of the correlations in (4.26); a situation of this sort should be classified with disordered structures. The degree of chaos of such structures depends on how rapidly correlation function (4.26) becomes uncoupled in accordance with a power law or exponentially. Structures with an exponential decay of the correlation function correspond to turbulence in a dynamic system.

A Penrose parquet apparently corresponds to case (4.27) with two basic incommensurate periods. All other cases require a careful analysis.

5. QUASICRYSTAL SYMMETRY

It is now clear that we have encountered a new type of symmetry, which has so far received little study. The tiling generator $\hat{M}_q$ and the average Hamiltonian $\overline{H}_q$ are possible means for expressing this symmetry. Here again we are naturally led to ask just how universal is a symmetry of the quasicrystal type and just where we can observe it, other than in real quasicrystals. Some possible applications will be mentioned in this section of the paper.

5.1. Hydrodynamic structures

The appearance of structures in various hydrodynamic flows is one of the earliest experimental observations. Among them, the most regular pattern is associated with convection cells, which can take the form of one-dimensional rollers or can produce a square or hexagonal network on the surface of a layer (Bénard cells). According to the general understanding of the appearance of structures, the reason for their appearance lies in various stages of the change in the state of a medium as it goes into turbulent motion. The more regular and simpler the structure, the higher is its symmetry, and the more ordered is the state of the medium. A turbulent state is the most homogeneous state (because of, for example, a local instability), and its symmetry is considerably higher than that of a structurally ordered medium. The greatest symmetry occurs in the case of highly developed turbulence. The path to the nucleation of turbulence is an exceedingly complicated one. It is determined not only by a complicated temporal sequence of bifurcations, which ultimately result in chaos and a continuous temporal spectrum, but also by a less complicated sequence of spatial changes in the structure of the medium, which lead to the appearance of spatially disordered structures. The latter circumstance gives rise to a continuous spectrum in terms of the *spatial* coordinates. The picture of the appearance of turbulence is thus a complicated path to the creation of spatial-temporal chaos. These ideas are being seen increasingly frequently in the current literature [58-61]

There have been many experimental and numerical studies of possible structural organizations of a medium (see, for example, the collections of reviews in Refs. 62–64, although the materials there do not come close to covering all the conferences on this subject). The structures which are easiest to analyze are the various two-dimensional structures which arise in problems of thermal convection or electrodynamic convection, which may also include parametric external excitation.[62,63,65-67] The list of problems of this sort is exceedingly long: the structure of foam, convection cells in the atmosphere of Jupiter,[68] structures in vortex arrays, structures in shear flows, etc. Along this path, structures with a quasicrystal type of symmetry may play an important role in hydrodynamic media in an analysis of the onset of turbulence.[21] Let us clarify why this may be so.

We turn to the two-dimensional hydrodynamics of an incompressible liquid. The equation of motion is

$$\frac{\partial}{\partial t}\left(\Delta\psi-\frac{1}{\mathrm{Re}}\Delta^2\psi\right)+\frac{\partial(\Delta\psi,\ \psi)}{\partial(x,\ y)}=0, \tag{5.1}$$

where ψ is the stream function ($v_x=\partial\Psi/\partial y$, $v_y=-\partial\Psi/\partial x$), Δ is the two-dimensional Laplacian, and Re is the Reynolds number.

We now consider ψ in the form

$$\psi_k=A(t)\sum_{j=1}^{q}\cos(k\mathbf{e}_j\mathbf{R}). \tag{5.2}$$

Expression (5.2) for the function ψ, which may be called a "quason," has the property

$$\Delta\psi_k+k^2\psi_k=0. \tag{5.3}$$

By virtue of (5.3), the nonlinear term in (5.1) vanishes identically, and we have

$$\dot{A}+\frac{1}{\mathrm{Re}}k^2A=0,$$

i.e.,

$$A(t)=A(0)\exp\left(-\frac{tk^2}{\mathrm{Re}}\right). \tag{5.4}$$

If, however, there is a pump, the quason may be a steady-state solution, and the question becomes one of determining the region in which such solutions are stable. This region may be related to various factors which have been neglected (compressibility, heat conduction, etc.). At the outset, however, we should not exclude solutions like (5.2), especially since they contain square and hexagonal networks as particular cases.

An equation analogous to (5.1) arises in the case of a rotating liquid[69]:

$$\frac{\partial}{\partial t}(u-\mathrm{Ro}^2\Delta u)+(\mathbf{v}_R\nabla)u=\Omega\,\mathrm{Ro}^4\frac{\partial(u,\ \Delta u)}{\partial(x,\ y)},$$

where u is the height of the liquid layer, Ω is the rotation frequency, $\mathbf{R}_0=(g\bar{u})^{1/2}/\Omega$ is the Rossby number, $\bar{u}$ is the average value of the height u, g is the acceleration due to gravity, $V_R=\mathbf{R}_0^2[\nabla\Omega,\mathbf{z}^0]$ is the Rossby drift velocity, and $\mathbf{z}^0$ is a unit vector along the rotation axis. The same equation corresponds to drift waves in a plasma,[70,71] where the role of Ω is played by the Larmor frequency in a magnetic field.

The studies carried out in Ref. 72 show that in the case of heat convection there is a stability region of quasons with an eightfold symmetry ($q=8$). The transition from regular structures to spatial chaos may be accompanied by a sequence of spatial bifurcations, and among them the development of structures with a quasicrystal symmetry may be quite probable. Regular structures with a complex order have been observed, for example, in experiments on the excitation of capillary ripple waves[60] and in a numerical analysis of the two-dimensional model described by the nonlinear Ginzburg-Landau equation.[73]

5.2. Structures in nature and in ornaments

How "often" can a quasicrystal type of symmetry be found in the world around us? As usual, this question presupposes an understanding of the extent to which this phenomenon is typical or easily realized. How often can a fairly random confluence of circumstances lead to the survival of structures with a quasicrystal symmetry? It turns out that such phenomena are not exceedingly rare. Kepler[74] noted certain regular properties in the structure of flowers, attempting to compare them structurally with snowflakes or honeycombs. He also pointed out a distinctive structural feature of pomegranate seeds, assuming it to be a consequence of certain conditions (forces) under which the seeds grew.

The structural order which is manifested in the arrangement of flowers, grains, leaves, etc. (e.g., in sunflower seeds and daisies), is called "phyllotaxy".[26] The regularities here have been discussed by botanists for a comparatively long time (Charles Bonnet, 1754). The objects of phyllotaxy usually have cylindrical and conical structures which are very strongly reminiscent of quasicrystals. The many analogies between phyllotaxy and quasicrystals were pointed out in Refs. 75 and 76. The most important of these analogies, however, may concern the properties of inflation and deflation. Through some simple partitionings and connections of the rhombi in a Penrose parquet (Fig. 12), one can convert it into exactly the same parquet, but now consisting of rhombi either larger (inflation) or smaller (deflation) in size.[38,48] The property of a self-similar structural transformation must be embodied in plants by virtue of their genetic code, although the structures themselves must have a similar self-similarity property. As a result, only certain structures are selected, and the limitations which stem from the need for a cylindrical symmetry immediately point out the reason for the appearance of elements of a quasicrystal type in phyllotaxy.[76]

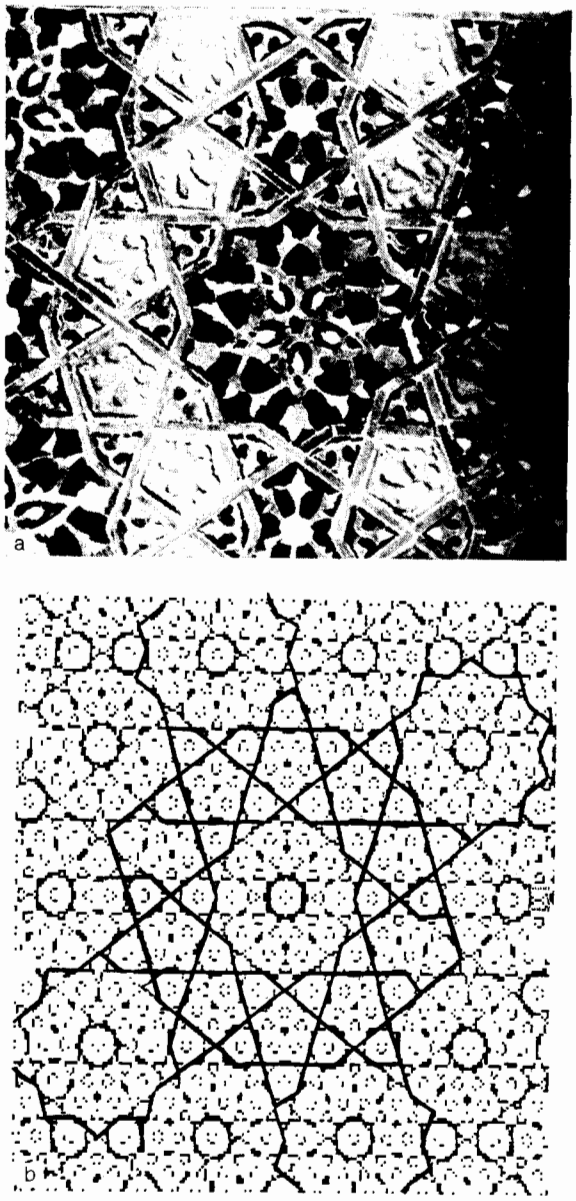

FIG. 27. a—Typical element of an Islamic ornament (in Tbilisi) with a decagonal element; b—its "deciphering" with the help of a relief with a fivefold symmetry.

As we have already mentioned, the products of ancient artisans and artists include samples of many methods for tiling a plane with very complex ornaments. Included here are all 17 methods for the periodic paving of a plane. Kepler also took up the problem of patterns, carrying out a fundamental study of mosaics in his work entitled *De Harmonice Mundi* (1619). Islamic paintings provide one of the richest examples of various tiling methods. A fivefold symmetry is a rare element and has been found in paintings in Alhambra palace in Granada, Spain. Various pentagonal and decagonal elements are also very common in many ornaments. Figure 27a shows a typical part of an Islamic pattern in which a regular decagon plays a basic role. These decagons are arranged on a regular rhombic lattice; the space between them is filled with suitable elements. The scheme for the formation of an ornament of this sort is shown in Fig. 27b through the use of a quasicrystal relief for $q = 5$ (Fig. 15a). This scheme illustrates a fairly important assertion: The reliefs generated by a quasicrystal symmetry open up new and exceptional opportunities for the creation of patterns, which the artists could hardly have imagined. An ornament with, say, a 17-fold symmetry could serve as an example of a situation in which, sad to say, the master has been surpassed by the computer.

CONCLUSION

We have reviewed known cases in which Hamiltonian systems contain a minimal chaos, manifested by the formation of universal regions of disrupted stochastic layers in place of the separatrices of the unperturbed dynamic system. A system of stochastic layers may tile the entire phase space, regardless of the strength of the perturbation and regardless of the dimensionality of the phase space greater than unity. As a result, a stochastic web arises, and an unbounded stochastic acceleration and diffusion of particles occurs along the channels of this web. For particles undergoing a random walk along the channels of the stochastic web, the adiabatic invariant may change substantially.

Another aspect of this phenomenon concerns the structural properties of the stochastic web, which may have a symmetry of a quasicrystal type. The formation of structures with a quasicrystal symmetry stems from an interaction of two types of symmetries: translational and rotational. Such

structures occupy an intermediate position between crystalline structures and amorphous structures. Quasicrystal symmetry is rather common in nature, being seen outside the realms of solid state physics and biology. The hydrodynamic equations also allow the existence of a class of solutions which have a quasicrystal symmetry. We can thus expect that such structures may arise in a transition to a state with spatial chaos.

These results show that we have encountered a universal phenomenon of nature, which is manifested in a variety of physical entities. It can be formulated briefly as follows: A weak interaction between mutually exclusive rotational and translational symmetries gives rise to a minimal chaos in regions with a quasicrystal structure.

We wish to thank Ya. G. Sinaĭ for useful comments.

APPENDICES

1. Determination of ΔE for a pendulum

The Hamiltonian

$$H=\frac{1}{2}p^2-\omega_0^2\cos x+\frac{\varepsilon\omega_0^2}{k}\cos(kx-\Delta\omega t) \qquad (A1.1)$$

corresponds to equation of motion (1.3). Integrating (1.6) over time, we find the following expression for the change in the energy of the unperturbed motion:

$$\Delta E=\int dt\varepsilon\omega_0^2\dot{x}\sin(kx-\Delta\omega t). \qquad (A1.2)$$

With $\varepsilon=0$, the motion along a separatrix is described by

$$x(t)=4\operatorname{arctg}\exp[\omega_0(t-t_n)]-\pi, \qquad (A1.3)$$

where t_n is the time at which the $x=0$ surface is intersected for the nth time. Substituting (A1.3) into the right side of (A1.2), and integrating over time, we find the change in the energy to be

$$\Delta E=2\varepsilon\omega_0^3\int_{-\infty}^{+\infty}dt\frac{1}{\operatorname{ch}\omega_0 t}\sin(4k\operatorname{arctg}e^{\omega_0 t}-\Delta\omega t-k\pi-\Delta\omega t_n). \qquad (A1.4)$$

We rewrite the right side of (A1.4) in the more compact form ($\nu\gg 1$)

$$\Delta E=-\varepsilon\omega_0^2 2^{2k+2}\sin(\Delta\omega t_n)\int_0^{\infty}d\tau\frac{\cos(\nu\tau)}{(\operatorname{ch}\tau)^{2k+1}}, \qquad (A1.5)$$

where $\nu=\Delta\omega/\omega_0$, and we evaluate the integral

$$\Delta E=-\frac{2^{4k+1}\varepsilon\omega_0^2}{\Gamma(2k+1)}\Gamma\left(k+\frac{1+i\nu}{2}\right)\times\Gamma\left(k+\frac{1-i\nu}{2}\right)\sin(\Delta\omega t_n). \qquad (A1.6)$$

In particular, if k is an integer, we have

$$\Delta E=-\pi\varepsilon\omega_0^2\frac{2^{4k+1}}{(2k)!}\frac{\sin(\Delta\omega t_n)}{\operatorname{ch}(\pi\nu/2)}\prod_{r=1}^{k}\left[\frac{\nu^2}{4}+\left(\frac{2r-1}{2}\right)^2\right]. \qquad (A1.7)$$

In the case $k=1$ we find the following exact expression from (A1.4):

$$\Delta E=-4\pi\varepsilon\omega_0^2\frac{\nu^2 e^{\pi\nu/2}}{\operatorname{sh}(\pi\nu)}\sin(\Delta\omega t_n). \qquad (A1.8)$$

2. Derivation of expression (2.15) for the thickness of a stochastic web

To evaluate the thickness of a stochastic web, we retain only the terms with $n=n_0\pm 1$ in sum (2.7). We restrict the analysis to particles with a fairly high energy ($k\rho_0\gg n_0$), and we use an asymptotic expansion of the Bessel function. The Hamiltonian of the problem then simplifies considerably:

$$H=H_0+V,\quad H_0=-\frac{\sigma\varepsilon\omega_0^2}{k}\left(\frac{2}{\pi k\rho_0}\right)^{1/2}\cos k\tilde{\rho}\cdot\cos\varphi,$$
$$V=-2\frac{\sigma\varepsilon\omega_0^2}{k}\left(\frac{2}{\pi k\rho_0}\right)^{1/2}\sin k\tilde{\rho}\cdot\sin\varphi\cdot\sin\frac{\varphi+\Delta\omega t}{n_0}, \qquad (A2.1)$$

where $\tilde{\rho}=\rho-\rho_0\ll\rho_0$, and $\sigma=\pm 1$, depending on the coordinate of the elliptical point.

The change in the energy of the average motion at $n_0\gg 1$ is given by the expression

$$\dot{H}_0=\frac{\partial H_0}{\partial\varphi}\dot{\varphi}+\frac{\partial H_0}{\partial I}\dot{I}=\frac{2n_0}{\pi}\varepsilon^2\omega_0\frac{1}{(k\rho_0)^2}(\cos 2k\tilde{\rho}-\cos 2\varphi)\cdot\sin\frac{\varphi+\Delta\omega t}{n_0}. \qquad (A2.2)$$

Motion along the separatrix is described by

$$\cos\varphi=\operatorname{ch}^{-1}\frac{(\pi/2)^{1/2}k\omega_0 n_0\varepsilon(t-t_n)}{(k\rho_0)^{3/2}}, \qquad (A2.3)$$

where t_n is the time at which the $\varphi=0$ surface is crossed for the nth time. Substituting the path of the motion of the particle from (A2.3) into the right side of (A2.2), and integrating over time, we find the change in the average energy over half an oscillation period:

$$\Delta E=-\frac{8\pi\omega_0^2 k\rho_0}{k^2 n_0}\exp\left[-\frac{(\pi/2)^{3/2}(k\rho_0)^{3/2}}{k\varepsilon n_0}\right]\sin(\omega_0 t_n). \qquad (A2.3')$$

The period of the oscillations of the particles in a cell near a separatrix is given by (2.14). Relations (2.14) and (A2.3) lead to a separatrix mapping which describes the dynamics of a particle as it moves along a stochastic web:

$$E_{n+1}=E_n-\frac{8\pi\omega_0^2(k\rho_0)}{k^2 n_0}\exp\left[-\frac{1}{k\varepsilon n_0}\left(\frac{\pi}{2}k\rho_0\right)^{3/2}\right]\sin\psi_n, \qquad (A2.4)$$
$$\psi_{n+1}=\psi_n+\left(\frac{\pi}{2}\right)^{1/2}\frac{2}{k\varepsilon n_0}\left(\ln\frac{4\varepsilon\omega_0^2}{k}\right)\left(\frac{2}{\pi k\rho_0}\right)^{1/2}\frac{1}{E_{n+1}},$$

where $\psi_n=\omega_0 t_n$ plays the role of a phase variable. Stochastic motion arises under the condition of local phase instability, $|d\Psi_{n+1}/d\Psi_n-1|>1$. We thus find an estimate of the thickness of a stochastic web: $|E|\leqslant E_s$, where

$$E_s=(2\pi)^{3/2}\frac{4\omega_0^2}{k^3\varepsilon n_0^2}(k\rho_0)^{5/2}\exp\left[-\frac{1}{k\varepsilon n_0}\left(\frac{\pi}{2}k\rho_0\right)^{3/2}\right]. \qquad (A2.5)$$

3. Stochastic acceleration of relativistic particles in a magetic field

The Hamiltonian H describing the interaction of a charged particle with a linearly polarized wave with a vector potential $\mathbf{A}=\mathbf{e}_y A\sin(kx-\omega t)$ in a transverse magnetic field $\mathbf{B}=\mathbf{e}_z B_0$ is

$$H=[m^2c^4+c^2p^2+e^2(B_0 x+A\sin(kx-\omega t))^2]^{1/2}. \qquad (A3.1)$$

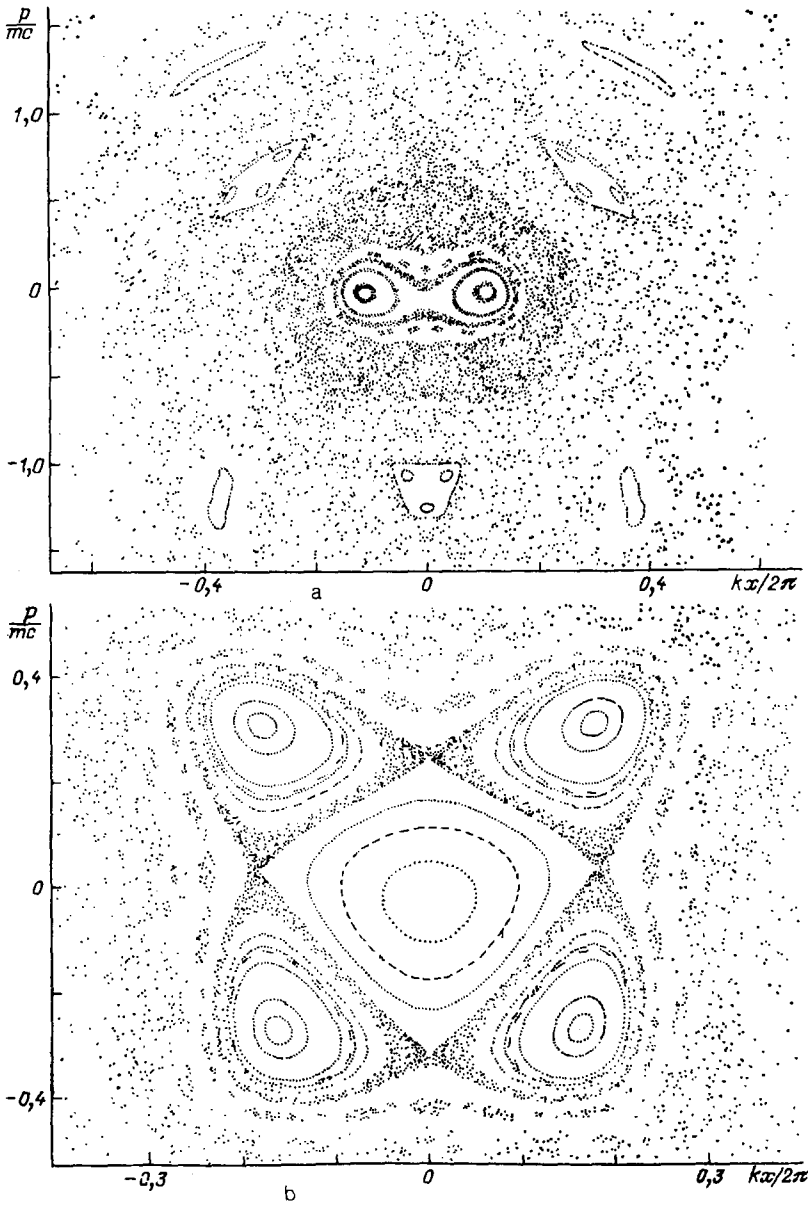

FIG. 28. Phase portraits of the system of equations (A3.2). a—$\omega/\omega_H = 2$, $eA/mc^2 = 0.1$; b—$\omega/\omega_H = 4$, $eA/mc^2 = 0.1$.

The corresponding canonical equations of motion are

$$\dot{x} = c^2 pH^{-1}, \quad \dot{p} = -e^2 H^{-1}[B_0 + kA\cos(kx - \omega t)] \times [B_0 x + A\sin(kx - \omega t)]. \qquad (A3.2)$$

Figure 28 shows the results of a numerical analysis[20] of system (A3.2). The numerical calculations show that the dynamics of high-energy particles with an energy $\mathscr{E} \gg mc^2$ is chaotic, and there is an unbounded stochastic acceleration of relativistic particles. For particles of sufficiently low energy, $\mathscr{E} \sim mc^2$, on the other hand, there are regions of regular motion. The dynamics of low-energy particles becomes particularly interesting in the case of a resonance between the frequency of the electromagnetic wave and the nonrelativistic cyclotron frequency: $\omega = n\omega_H$. A system of relatively large stability islands appears on the phase portrait at low energies. In Fig. 26a, which corresponds to the case $\omega = 2\omega_H$, we also see some stability islands, which correspond to cyclotron resonances of second, third, and fourth orders. In the regions between stability islands, stochastic layers form. At small values of the parameter eA/mc^2, the stochastic layers surrounding cyclotron resonances are separated from each other by invariant curves. As the energy of the particles increases, the invariant curves between layers disappear, and something reminiscent of a stochastic web arises (Fig. 28b). This web, however, quickly breaks up as the energy is increased, because of a pronounced nonlinearity of the motion of a relativistic particle in a magnetic field, and the particles are in a regime of unbounded stochastic acceleration. The threshold particle energy $\mathscr{E}_{\text{thr}}$, at which stochastic acceleration arises, is[20]

$$\mathscr{E}_{\text{thr}} = \frac{mc^2}{16^3}\left(\frac{\omega_H}{\omega}\right)^4\left(\frac{mc^2}{eA}\right)^3. \qquad (A3.3)$$

Diffusion in the phase plane of particles with an energy above threshold (A3.3) can be described in the standard way by a Fokker-Planck-Kolmogorov equation. To derive a diffusion equation, we take the approach of Ref. 7, switching to the action-angle variables of the unperturbed problem, (J, θ), in the Hamiltonian (A3.1). The unperturbed problem corresponds to the free revolution of a relativistic particle in a magnetic field:

$$x = \rho \sin\theta, \quad p = \rho m\omega_H \cos\theta, \tag{A3.4}$$

where $\rho = (2cJ/eB_0)^{1/2}$ is the Larmor radius. In terms of the new variables, the Hamiltonian (A3.1) becomes

$$H(J, \theta, t) = \Big[H_0^2 + 2e^2B_0A\rho \sin\theta \cdot \sin(k\rho\sin\theta - \omega t) - \frac{e^2A^2}{2}\cos(2k\rho\sin\theta - 2\omega t)\Big]^{1/2}, \tag{A3.5}$$

where

$$H_0(J) = \Big(m^2c^4 + \frac{e^2A^2}{2} + 2ceB_0J\Big)^{1/2} \tag{A3.6}$$

is the Hamiltonian of the unperturbed problem. For particles which have a sufficiently high energy $\mathscr{E} \gg eA$, expression (A3.6) simplifies slightly and can be written in the form

$$H(J, \theta, t) = H_0 - \frac{e^2B_0A\rho}{H_0}\sum_{n=-\infty}^{+\infty} J_n'(k\rho)\cos(n\theta - \omega t), \tag{A3.6}$$

where $J_n'(k\rho)$ is the derivative of the Bessel function with respect to its argument. The motion of particles with an energy above the threshold energy in (A3.3) is chaotic and is characterized by a rapid mixing of phases and a slower diffusion over action. The diffusion equation, which incorporates the finite correlation uncoupling time in the approach of Ref. 7, is

$$\frac{\partial f}{\partial t} = \frac{\partial}{\partial J}D(J)\frac{\partial f}{\partial J}, \tag{A3.8}$$

where $D(J)$ is the diffusion coefficient, given by

$$D(J) = \Big(\frac{e^2B_0A\rho}{2H_0}\Big)^2 \sum_{m=-\infty}^{+\infty} m^2J_m'^2(k\rho) \times \int_0^\infty d\tau \exp\Big[-i(m\Omega - \omega)\tau - \frac{\tau}{\tau_c}\Big] + \text{c.c.} \tag{A3.9}$$

Here $\Omega = \partial_0 H/\partial J$ is the nonlinear frequency of the unperturbed motion, and τ_c is the time scale of the uncoupling of the phase correlations.[20] Evaluating the integral over time on the right side of (A3.9), we find

$$D(J) = \Big(\frac{e^2B_0A\rho}{2H_0}\Big)^2 (i/\Omega)\sum_{m=-\infty}^{+\infty}\Big[m - \frac{\omega}{\Omega} + \frac{i}{\Omega\tau_c}\Big]^{-1} - \Big[m - \frac{\omega}{\Omega} - \frac{i}{\Omega\tau_c}\Big]^{-1} m^2J_m'^2(k\rho). \tag{A3.10}$$

The series on the right side of (A3.10) can be summed with the help of the identity

$$\sum_{m=-\infty}^{+\infty}\frac{J_{m+p}(a)J_m(a)}{m-q} = -\frac{\pi}{\sin\pi q}J_{p+q}(a)J_{-q}(a). \tag{A3.11}$$

As a result we find the following expression for the diffusion coefficient in the limit $(\Omega\tau_c \to 0)$:

$$D(J) = \frac{\pi}{2}\Big(\frac{e^2B_0A\rho}{H_0}\Big)^2\frac{\omega^2}{\Omega^3}J_{\omega/\Omega}'^2(k\rho). \tag{A3.12}$$

If the phase velocity of the electromagnetic wave is equal to the velocity of light, $\omega = kc$, expression (A3.12) simplifies at high energies, and Eq. (A3.8) becomes

$$\frac{\partial f}{\partial t} = \nu_0\frac{\partial}{\partial J}J^{5/6}\frac{\partial f}{\partial J}, \tag{A3.13}$$

where $\nu_0 = \xi A^2\omega^{2/3}e^{7/6}B_6^{-5/6}c^{-5/6}$, and the numerical coefficient is

$$\zeta = \frac{\pi 2^{7/6}3^{-2/3}}{\Gamma^2(1/3)}.$$

A solution of Eq. (A3.13) with initial condition $f(t=0) = f_0(J)$ is

$$f(J, t) = \Big(\frac{6J^{1/12}}{7\nu_0 t}\Big)\exp\Big(-\frac{36J^{7/6}}{49\nu_0 t}\Big) \times \int_0^\infty dJ'J'^{1/12}\exp\Big(-\frac{36J'^{7/6}}{49\nu_0 t}\Big) \times I_{-1/7}\Big(\frac{72(JJ')^{7/12}}{49\nu_0 t}\Big)f_0(J'). \tag{A3.14}$$

at large times t, solution (A3.14) becomes a self-similar solution, "forgetting" about the initial conditions:

$$f(J, t) = \frac{(6/7)^{5/7}}{\Gamma(6/7)}\frac{N}{(\nu_0 t)^{6/7}}\exp\Big(-\frac{36J^{6/7}}{49\nu_0 t}\Big), \tag{A3.15}$$

where $N = \int dJf$ is the density of particles. The energy distribution of the particles is also of a self-similar form:

$$f(\mathscr{E}, t) \sim \mathscr{E}t^{-6/7}\exp\Big(-\frac{\text{const}\cdot\mathscr{E}^{7/3}}{t}\Big). \tag{A3.16}$$

Consequently, the average energy of the particles, $\langle\mathscr{E}\rangle$, increases over time in accordance with

$$\langle\mathscr{E}\rangle \sim t^{3/7}. \tag{A3.17}$$

[1)] Or on a surface which is the product of an $(N-m)$-dimensional torus and an m-dimensional cylinder.

[1] H. Poincaré, *Les méthodes nouvelles de la mechanique céleste* **3**, Gauthier-Villars, Paris, 1899. [Russ. transl. in Selected Works, Vol. 1, Nauka, M., 1971].
[2] V. K. Mel'nikov, Dokl. Akad. Nauk SSSR **148**, 1257 (1963) Sov. Math. Dokl. **148**, 266 (1963)].
[3] N. N. Filonenko, R. Z. Sagdeev, and G. M. Zaslavsky, Nucl. Fusion **7**, 253 (1967).
[4] G. M. Zaslavskii and N. N. Filonenko, Zh. Eksp. Teor. Fiz. **54**, 1590 (1968) [Sov. Phys. JETP **27**, 851 (1968)].
[5] G. M. Zaslavskiĭ, M. Yu. Zakharov, R. Z. Sagdeev, D. A. Usikov, and A. A. Chernikov, Zh. Eksp. Teor. Fiz. **91**, 500 (1986) [Sov. Phys. JETP **64**, 294 (1986)].
[6] V. I. Arnol'd, V. V. Kozlov, and A. I. Neĭshtadt, "Mathematical aspects of classical and celestial mechanics," in: Scientific and Technological Progress. Series on Current Problems in Mathematics, Vol. 3 (In Russian), VINITI Akad. Nauk SSSR, Moscow, 1985.
[7] G. M. Zaslavskiĭ, Stochastic Nature of Dynamic Systems (In Russian), Nauka, M., 1984.
[8] B. V. Chirikov, Phys. Rep. **52**, 263 (1979).
[9] G. M. Zaslavskiĭ, Zh. Eksp. Teor. Fiz. **88**, 1984 (1985) [Sov. Phys. JETP **61**, 1176 (1985)].
[10] S. M. Ulam, *A Collection of Mathematical Problems*, Interscience, N. Y., 1960. [Russ. transl. Nauka, M., 1964.]
[11] V. I. Arnol'd, *Mathematical Methods of Classical Mechanics* (Graduate Texts in Mathematics, Vol. 60), Springer-Verlag, N. Y., 1978. [Russ. original, Nauka, M., 1974].
[12] V. I. Arnol'd, Dokl. Akad. Nauk SSSR **156**, 9 (1964) Sov. Math. Dokl. **156**, 581 (1964)].
[13] C. F. Karney, Phys. Fluids **21**, 1584 (1978); **22**, 2188 (1979).
[14] S. Riyopoulos, T. M. Antonsen, and E. Ott, Phys. Fluids **27**, 184 (1984).
[15] A. Fukuyama, H. Momota, R. Itatani, and T. Takizuka, Phys. Rev. Lett. **38**, 701 (1977).
[16] A. J. Lichtenberg and M. A. Lieberman, *Regular and Stochastic Motion*, Springer-Verlag, N. Y., 1983 [Russ. transl., Mir, M., 1984].
[17] R. Z. Sagdeev and V. D. Shapiro, Pis'ma Zh. Eksp. Teor. Fiz. **17**, 389 (1973) [JETP Lett. **17**, 279 (1973)].

[18]R. Z. Sagdeev and G. M. Zaslavsky, in: Nonlinear Phenomena in Plasma Physics and Hydrodynamics (ed. R. Z. Sagdeev), Mir, M., 1986.
[19]A. A. Chernikov, M. Ya. Natenzon, B. A. Petrovichev, R. Z. Sagdeev, and G. M. Zaslavsky, Phys. Lett. **A122**, 39 (1987).
[20]G. M. Zaslavskiĭ, M. Ya. Natenzon, B. A. Petrovichev, R. Z. Sagdeev, and A. A. Chernikov, Zh. Eksp. Teor. Fiz. **93**, 881 (1987) [Sov. Phys. JETP **66**, 496 (1987)].
[21]G. M. Zaslavskiĭ, M. Yu. Zakharov, R. Z. Sagdeev, D. A. Usikov, and A. A. Chernikov, Pis'ma Zh. Eksp. Teor. Fiz. **44**, 349 (1986) [JETP Lett. **44**, 451 (1986)].
[22]L. D. Landau and B. M. Lifshitz, *Statistical Physics*, Addison-Wesley, Reading, Mass., 1969 [Russ. original, Nauka, M., 1964].
[23]B. Mandelbrot, *The Fractal Geometry of Nature*, Freeman, San Francisco, 1982.
[24]R. S. Mackay, J. D. Meiss, and I. C. Percival, Physica **D13**, 55 (1984).
[25]A. A. Chernikov, R. Z. Sagdeev, D. A. Usikov, M. Yu. Zakharov, and G. M. Zaslavsky, Nature **326**, 559 (1987).
[26]H. Weyl, *Symmetry*, Princeton Univ. Press, Princeton, 1952 p. 77 [Russ. transl., Nauka, M., 1968].
[27]D. A. Klarner (editor), *The Mathematical Gardner*, Prindle, Weber, and Schmidt, Boston, 1981 [Russ. transl., Mir, M., 1983].
[28]M. Senechal and G. Fleck (editors), *Patterns of Symmetry*, Univ. of Massachusetts Press, Amherst, 1977 [Russ. transl., Mir, M., 1980].
[29]H. S. M. Coxeter, *Introduction to Geometry*, Wiley, N. Y., 1961, 2nd ed. 1969. [Russ. transl., Nauka, M., 1966].
[30]J. L. Locher (ed.), *The World of M. C. Escher*, Abrahams, N. Y., 1977.
[31]S. Aubry, J. Phys. (Paris) **44**, 147 (1983).
[32]P. I. Belobrov, V. V. Beloshapkin, G. M. Zaslavskiĭ, and A. G. Tret'yakov, Zh. Eksp. Teor. Fiz. **87**, 310 (1984) [Sov. Phys. JETP **60**, 180 (1984)].
V. L. Pokrovsky and A. L. Talapov, *Theory of Incommensurate Crystals*, Hardwood Acad. Publ., New York, 1984.
[34]E. Schrödinger, *What is Life?*, Cambridge Univ. Press, 1972. [Russ. transl., Atomizedat., M., 1972].
[35]A. L. Mackay, Kristallografiya **26**, 910 (1981) [Sov. Phys. Crystallogr. **26**, 517 (1981)]; Physica **A114**, 609 (1982).
[36]A. L. Mackay, J. Phys. (Paris) **47**, C3, Suppl. au Nr. 7, 153 (1986).
[37]R. Penrose, Bull. Inst. Math. Appl. **10**, 266 (1974).
[38]M. Gardner, Sci. Am. **236**, 110 (1977).
[39]D. Shechtman, I. Blech, D. Gratias, and J. W. Cahn, Phys. Rev. Lett. **53**, 1951 (1984).
[40]International Workshop on Aperiodic Crystals, J. Phys. (Paris) **47**, C3, Suppl. au Nr. 7 (1986).
[41]N. G. DeBruijn, Kon. Nederl. Akad. Wetesch. Proc. **A84**, 38, 53 (1981).
[42]P. Kramer and R. Neri, Acta Crystallogr. Sect. A. **40**, 580 (1984).
[43]V. Elser, Phys. Rev. **B32**, 4892 (1985).
[44]P. A. Kalugin, A. Yu. Kitaev, and L. S. Levitov, Pis'ma Zh. Eksp. Teor. Fiz. **41**, 119 (1985) [JETP Lett. **41**, 145 (1985)].
[45]M. Duneau and A. Katz, Phys. Rev. Lett. **54**, 2688 (1985).
[46]N. G. De Bruijn, J. Phys. (Paris) **47**, C3, Suppl. au Nr. 7, 9 (1986).
[47]F. Gahler and J. Phyner, J. Phys. **A19**, 267 (1986).
[48]D. Levine and P. J. Steinhardt, Phys. Rev. **B84**, 596 (1986).
[49]P. Bak Phys. Rev. **B32**, 5764 (1985).
[50]D. Levine and P. J. Steinhardt, Phys. Rev. Lett. **53**, 2477 (1984).
[51]D. Levine, J. Phys. (Paris) **47**, C3, Suppl. au Nr. 7, 125 (1986).
[52]D. R. Nelson and S. Sachdev, Phys. Rev. **B32**, 689 (1985).
[53]D. R. Nelson and S. Sachdev, Phys. Rev. **B32**, 4592 (1985).
[54]G. M. Zaslavskiĭ, R. Z. Sagdeev, D. A. Usikov, A. A. Chernikov, Preprint No. 1229, Institute of Space Research, Academy of Sciences of the USSR, Moscow; Phys. Lett. **A125**, 101 (1987).
[55]T. Ishimasa, H. U. Nissen, and Y. Fukano, Phys. Rev. Lett. **55**, 511 (1985).
[56]R. Mosseri and J. P. Sadoc, J. Phys. (Paris) **47**, C3, Suppl. au Nr. 7, 281 (1986).
[57]T. C. Choy, Phys. Rev. Lett. **55**, 2915 (1985).
[58]R. Z. Sagdeev, D. A. Usikov, and G. M. Zaslavsky, *Nonlinear Physics*, Hardwood Acad. Publ., N. Y., 1988.
[59]A. C. Newell, in: *Perspectives in Nonlinear Dynamics* (ed. M. F. Shlesinger *et al.*), World Scientific, Singapore, 1986, p. 38.
[60]A. B. Ezerskii, M. I. Rabinovich, V. P. Reutov, and I. M. Starobinets, Zh. Eksp. Teor. Fiz. **91**, 2070 (1986) [Sov. Phys. JETP **64**, 1228 (1986)].
[61]H. Chate and P. Manneville, Phys. Rev. Lett. **58**, 112 (1987).
[62]J E. Wesfreid and S. Zaleski (editors), *Cellular Structures in Instabilities*, Springer-Verlag, New York, 1984.
[63]M. F. Shlesinger *et al.* (editors), *Perspectives in Nonlinear Dynamics*, World Scientific, Singapore, 1986.
[64]Physica **D23**, No. 1–3 (1986).
[65]J. P. Gollub, in: *Perspectives in Nonlinear Dynamics* (ed. M. F. Shlesinger *et al.*), World Scientific, Singapore, 1986, p. 24.
[66]A. B. Ezerskiĭ, P. N. Korotkin, and M. I. Rabinovich, Pis'ma Zh. Eksp. Teor. Fiz. **41**, 129 91985) [JETP Lett. **41**, 157 (1985)].
[67]A. V. Gaponov-Grekhov, A. S. Lomov, and M. I. Rabinovich, Pis'ma Zh. Eksp. Teor. Fiz. **44**, 242 (1986) [JETP Lett. **44**, 310 (1986)].
[68]G. P. Williams, J. Atm. Sci. **35**, 1399 (1978).
[69]J. G. Charney, Geophys. Publ. **17**, 3 (1948).
[70]A. Hasegawa, Adv. Phys. **34**, 1 (1985).
[71]M. V. Nezlin, Usp. Fiz. Nauk **150**, 3 (1986) [Sov. Phys. Usp. **29**, 807 (1986)].
[72]B. A. Malomed, A. A. Nepomnyashchiĭ, and M. I. Tribel'skiĭ, Pis'ma Zh. Tekh. Fiz. **13**, 1165 (1987) [Sov. Tech. Phys. Lett. **13**, 487 (1987)].
[73]I. S. Aranson, A. V. Gaponov-Grekhov, M. I. Rabinovich, A. V. Rogal'skiĭ, and R. Z. Sagdeev, "Lattice models in the nonlinear dynamics of nonequilibrium media," Preprint No. 163, Institute of Applied Physics, Academy of Sciences of the USSR, Gor'kiĭ, 1987.
[74]J. Kepler, *The Six-cornered Snowflake*, Clarendon Press, Oxford, 1966. [Russ. transl., Nauka, M., 1982].
[75]N. Rivier, R. Occelli, J. Pantaloni, and A. J. Lissowski, J. Phys. (Paris) **45**, 49 (1984).
N. Rivier, J. Phys. (Paris) **47**, C3, Suppl. au Nr., 299 (1986).
[77]A. V. Shubnikov and V. A. Koptsik, *Symmetry in Science and Art*, Plenum Press, N. Y., 1974 [Russ. original Nauka, M., 1972.]
[78]V. E. Korepin, Quasiperiodic Tilings and Quasicrystals. Notes of Scientific Seminars of the Leningrad Branch of the V. A. Steklov Mathematics Institute, Vol. 155 (In Russian), Nauka, 1986, p. 116. [Transl. expected in a future issue of J. Sov. Math.]
[79]T. C. Lubensky, J. E. S. Socolar, P. J. Steingardt, P. A. Bancel, and P. A. Heiney, Phys. Rev. Lett. **57**, 1440 (1986).
[80]B. Grunbaum and G. C. Shepard, *Tilings and Patterns*, Freeman, San Francisco, 1986.
[81]N. Wang, H. Chen, K. H. Kuo, Phys. Rev. Lett. **59**, 1010 (1987).
[82]S. Ushiki, Physica **D4**, 407 (1982).
[83]V. I. Arnol'd, Usp. Mat. Nauk **42**, 139 (1987).

Translated by Dave Parsons